Nanoscale

REVIEW

View Article Online
View Journal | View Issue

Cite this: *Nanoscale*, 2014, **6**, 4438

Mesoporous nano/micro noble metal particles: synthesis and applications

Shengchun Yang* and Xiao Luo

Received 27th December 2013
Accepted 4th February 2014

DOI: 10.1039/c3nr06858g

www.rsc.org/nanoscale

The morphology, size and composition often govern the physical and chemical properties of noble metal units with a size in the nano or micro scale. Thus, the controlled growth of noble metal crystals would help to tailor their unique properties and this would be followed by their practical application. Mesoporous nano/micro noble metal units are types of nanostructured material that have fascinating properties that can generate great potential for various applications. This review presents a general view on the growth mechanisms of porous noble metal units and is focused on recent progresses in their synthetic approaches. Then, their potential applications in the field of drug delivery, cell imaging and SERS substrates, as well as fuel cell catalysts are overviewed.

1. Introduction

Porous materials, which are composed of an interconnected network of pores or voids,[1–5] are normally characterized by low density and a high specific surface area. For most chemists engaged in catalysis research, the most attractive qualities of porous materials should be their high specific surface area, superior connectivity and mass diffusion properties and, sometimes, good chemical and physical stability. This is because the porous characteristics endow them with the ability to interact with atoms, ions and molecules not only at their surfaces, but throughout the bulk of the material.[6] In addition, the partitions between nanoparticles (NPs) by the pore structures greatly inhibit particle growth as well as reducing particle aggregation. Thus, porous materials are generally chosen as the supports for catalysts or used directly as catalysts in some chemical reactions. Typical examples are supported noble metal NPs on porous materials, such as Au, Pt and Pd NPs loaded on zeolites for photooxidation,[7] hydrogenation/hydrodeoxygenation,[8,9] CO oxidation,[10] ring opening, and cross-coupling reactions.[11] In these catalytic reactions, the noble metal NPs supported on porous substrates exhibit significantly improved catalytic activity, efficiency and stability compared with their unsupported counterparts.

However, in some cases, the reduction of the size of porous particles to the nanoscale offers an additional potential to optimize the performance of porous solids not only in

MOE Key Laboratory for Non-equilibrium Synthesis and Modulation of Condensed Matter, State Key Laboratory for Mechanical Behavior of Materials, School of Science, Xi'an Jiaotong University, Shann Xi, 710049, People's Republic of China. E-mail: ysch1209@mail.xjtu.edu.cn; Fax: +86-29-82665995; Tel: +86-29-82663034

Professor Shengchun Yang received a BS degree from Shaanxi Normal University in 2002, an MS degree from Kunming Institute of Precious Metals in 2005, and a PhD degree in Physics from Xi'an Jiaotong University (XJTU), in 2008. Between 2007 and 2008, he worked at the University of Rochester as a research scholar. He is currently a Professor in the Department of Material Physics at XJTU. His main research interests are the synthesis and assembly of nanomaterials, and materials for energy applications such as batteries, fuel cells and photocatalysis.

Xiao Luo received his BS degree in Physics from Shaanxi Normal University in 2010. He is currently pursuing his MS degree under the supervision of Professor Shengchun Yang at Xi'an Jiaotong University. His research focuses on the synthesis and applications of silver phosphate and porous noble metal materials.

traditional catalytic applications but also in the field of biomedicine.[12] For example, isolated noble metal porous units engineered to the micro- or nano-scaled size have shown potential for drug delivery,[13–16] cell imaging,[17] fuel cells,[18,19] SERS[20–22] and virus-elimination,[23] due to their unique properties of large specific surface area, high porosity, good mass conductivity and relatively smaller sizes. The porous structure can enlarge greatly the active sites and enhance the mass transition of the fuel molecules that can enhance greatly their activity and durability in fuel cell applications. Similarly, the porous and hollow structure in particles can provide an enlarged capacity for drug loading and multichannels for drug delivery. In addition, the porous structure can create a rough surface which may generate high density "hot spots" to improve their SERS performance.

In recent years, the shape, size and facets of noble metal particles have already been extensively studied.[24–26] The noble metal particles, such as Au, Ag, Pt and Pd possess a range of unique properties, which can be controlled by varying their size and morphology.[27–31] As for the porous noble metal nano/microparticles, various methods have been developed to achieve this special structure with controllable porosity, morphology and size. Among them, the most popular approach is the template method which can be separated into two major steps: the synthesis of template and the growth of target materials. The most important factor in controlling the morphology of the final products is the shape or morphology of the starting template. The porous structure in the final product can be produced through a one- or multi-step reaction. The porous units synthesized by template strategies can hold a well-defined size, shape and configuration. In addition, some templateless strategies, including chemical etching, direct synthesis in solution, overgrowth on existing anisotropic crystals, *et al.*, were also developed.

In this review, we will start with a description of general approaches and mechanism of the synthesis of porous noble metal units. Next, the fundamental properties and applications of porous noble metal units will be reviewed.

2. General mechanisms and synthesis methods of the porous noble metal units

2.1 Template method

There are a variety of interesting benefits associated with template method, because it can fabricate materials with certain shapes and structures which are hard to obtain by other approaches.[32] In realistic synthesis, any substance with nanostructured features can be selected as a potential template, such as metal, metal oxides, nonmetals and even polymers. The template method is a facile and effective strategy towards the synthesis of porous units with controlled size and morphology, because the use of pregrown templates allows the morphology and porosity of the resultant particles to be engineered facilely.[33] A proper reaction needs to be designed for the direct synthesis of target materials on the template. Then, if necessary, a suitable route must be conducted to remove the initial template without breaking the structure of the product. Basically, the general mechanisms for the synthesis of noble metal porous units involved in the template methods mainly include the Kirkendall effect occurring in the galvanic replacement reactions, the volume shrinkage induced by the formation of the pores and growing the crystals along the three-dimensional microporous structure comprising channels and voids in polymers or zeolites.

2.1.1 Kirkendall effect and galvanic reaction. Atoms can migrate through the interface of coupled materials. In the past, it was believed that the atomic diffusion in metals and alloys was at the same diffusion rate. Kirkendall for the first time suggested in 1942 a motion boundary of the layers between two metals that occurs as a consequence of the difference in diffusion rates of the metal atoms.[34] In 1947, Smigelkas and Kirkendall reported that the different diffusion rates of these two species at an elevated temperature could cause the movement of the interface between a diffusion couple.[35] One of the primary consequences of the Kirkendall effect is the formation of voids at the boundary interface. These are referred to as Kirkendall voids. As shown in Fig. 1, if we assume the diffusion rates of the two species are different ($J_A > J_B$), there will be a flow of matter past the interface. The whole material therefore translates along the interface as diffusion proceeds because the flux of A is larger than that of B, causing a net flow of matter translation from A to B. This process will induce an equal and opposite flow of vacancies, causing a condensation of the vacancies and leading to the formation of the pores and voids inside A (Fig. 1).

In 2004, Alivisatos *et al.* first reported the nanoscale Kirkendall effect for the formation of cobalt sulfide nanocrystals with a hollow interior.[37] They fabricated hollow nanocrystals by using colloidal cobalt reacted with selenium. During the reaction, the diffusion of cobalt and selenium atoms in opposite directions leads to the cobalt atoms diffusing out to the shell and vacancies diffusing inward, thus forming hollow CoSe alloy NPs. Since this report, a number of hollow structures have been extensively explored using the Kirkendall effect.[36] Typical examples should be the synthesis of hollow and porous noble metal nanostructures through the galvanic replacement

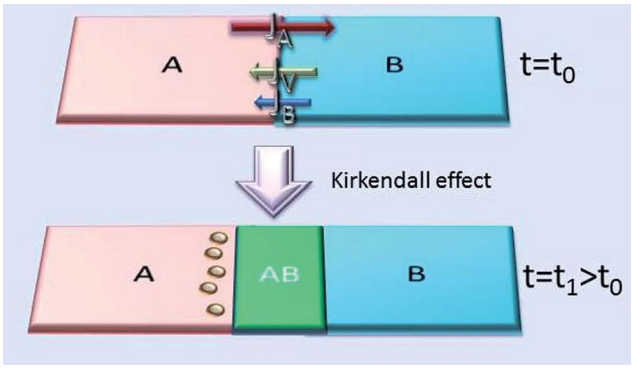

Fig. 1 Schematic mechanisms of the Kirkendall effect. (Adapted and revised with permission from ref. 36, copyright 2013, American Association for the Advancement of Science.)

reaction. The difference in redox potentials between the two metal species provide the kinetics for the reaction causing it to occur spontaneously, in which the metal species with lower electrochemical potential serves as the anode while the other metal, with higher potential, is the cathode. During the galvanic replacement reaction, the noble metal ions are reduced and deposited onto the surface of the templates. In this process, the first metal is consumed continuously from the core leading to the formation of a hollow or porous interior.

Ag is an ideal and widely reported template for the synthesis of porous or hollow noble metal nanoparticles with various morphologies,[38–44] because Ag can be replaced by other noble metals, such as gold,[42,45,46] platinum[47–49] and palladium[50] *via* the galvanic reaction. Gonzalez *et al.* demonstrated a synthetic route for the production of polymetallic hollow nanoparticles with very different morphologies and compositions, obtained by the simultaneous or sequential action of galvanic replacement and the Kirkendall effect, as well as pitting, etching, and dealloying corrosion processes.[51] As shown in Fig. 2, by controlling carefully the reaction and diffusion processes, they synthesized spherical, cubic, and cylindrical Au–Ag and Au–Ag–Pd bi/tri-metallic porous/hollow nanostructures. The galvanic replacement between Ag and Au(III) ions causes the formation of pinholes on the walls. Once the cavity is formed by galvanic replacement and its surface covered by a gold layer, Kirkendall cavities will form because a thin film of silver between two layers of gold will provide intermetallic diffusion coupling.

Besides formation of the voids in inner particles, Lu and co-workers found that the void spaces and porous walls with controlled number can be produced around the Ag template *via* a tailored galvanic replacement reaction.[52] Four different shapes, *i.e.*, nanoboxes, heterodimers, multimers and nanopopcorns were prepared with minor modification in the chemical environment, such as the concentration of HCl in solution (Fig. 3). The use of HCl in the galvanic reaction was considered to cause a rapid precipitation of AgCl, which grew on the surface of Ag NCs and acted as a removable secondary template for the deposition of Pt. The number of nucleation sites for AgCl was tailored by controlling the amount of HCl added to the Ag NCs or by introducing PVP to the reaction. After removal of the AgCl cores deposited on the surface of the Ag template, hollow or porous Pt "bubbles" were formed.

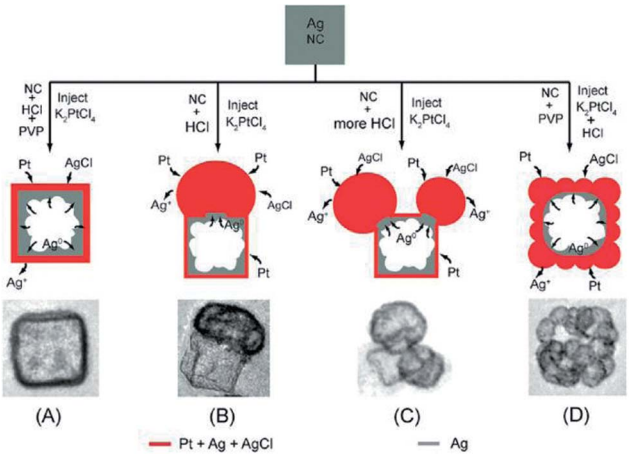

Fig. 3 Illustration of SEM images and the formation of Pt/Ag (A) nanoboxes, (B) heterodimers, (C) multimers, and (D) popcorn-shaped nanoparticles from the GRR between Ag nanocrystals and K_2PtCl_4 in the presence of HCl. (Adapted with permission from ref. 52, copyright 2011, American Chemical Society.)

By controlling the reaction conditions, the galvanic replacement reaction can be used to fabricate the Au–Ag alloy nanoframe without requiring a conventional Ag removal step. Hong *et al.* demonstrated a "one-pot" strategy to produce Au–Ag nanoframes with additional oxidation etchant, in which the $AgNO_3$, CuCl, and $HAuCl_4$ were added sequentially to an octadecylamine solution.[53] As shown in Fig. 4, the truncated polyhedral silver nanoparticles formed first and then changed into octahedral Au–Ag nanoframes. The nanoframes have 12 sides and all of the eight {111} faces are empty. The formation of the nanoframes was attributed to the difference in facet energy, in which the surface energies of crystal facets follows the order of $\gamma\{111\} < \gamma\{100\} < \gamma\{110\}$. Ag in the stable {111} faces was easier to be oxidized. Thus the etching reaction would take place on all eight of the {111} faces, leading to the formation of

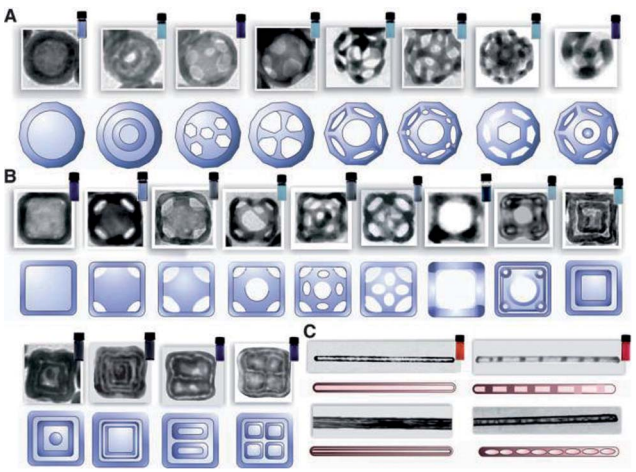

Fig. 2 The porous/hollow noble metal nanoparticles reported in ref. 46 with (A) spherical, (B) cubic, and (C) cylindrical topologies. (Adapted with permission from ref. 51, copyright 2011, American Association for the Advancement of Science).

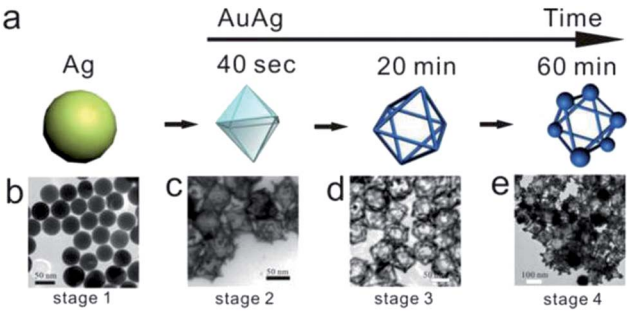

Fig. 4 (a) Schematic illustration of the deduced process of Au–Ag octahedral nanoframe formation. (Adapted with permission from ref. 53, copyright 2012, American Chemical Society.)

nanoframes. Detsi *et al.* demonstrated that the bimetallic Au–Ag alloy nanoparticles with high porosity through their entire bulk (rather than nanocages) could form, when the galvanic replacement reaction between Ag atoms and $AuCl_4^-$ ions took place directly during the growth of Ag nanoparticles.[54] Recently, Au–M (M = Au, Pd, and Pt) core–shell nanostructures with porous shells were prepared through the galvanic displacement reaction using Au–Ag core–shell nanoparticles as a sacrificial template.[55] Song and coworkers[56] found that the higher reduction potential of Au compared to Ag, Pd, and Pt could help to produce a hollow Au core with a Pd or Pt shell. Continuous and highly crystalline shell growth was observed in Au@Pd core–shell NPs, while a porous structure was observed in Au@Pt core–shell NPs. Additionally, when the silver flowers composed of thin nanosheets were used as a sacrificial template, as shown in Fig. 5, the mesoporous flower-like Pt and PtAg alloy nanostructures were prepared, rather than formation of the hollow interior in particles.[57] The $Pt_{45}Ag_{55}$ and $Pt_{72}Ag_{28}$ were obtained by the galvanic displacement of the Ag mesoflowers with chloroplatinic acid for different reaction times. The pure Pt mesoflowers were synthesized by selective removal of rudimental Ag with nitric acid treatment.

Palladium nanoparticles were also selected as the sacrificial template for the synthesis of Pt hollow/porous nanoparticles, since the difference in the reduction potential between $PtCl_4^{2-}$ and $PdCl_4^{2-}$ was 0.2 V.[58] Thus when Pd NPs were used as sacrificial templates, the Pt ion precursors could be reduced to metal, although they showed a less efficient and slow reaction compared to the case where Ag NCs were employed as templates. Han *et al.* reported a method of synthesizing Pd–Pt alloy nanoparticles with hollow structures, such as nanocages with porous walls, dendritic hollow structures and Pd@Pt core–shell dendritic nanocrystals by a galvanic replacement method with uniform Pd octahedral and cubic nanocrystals as sacrificial templates.[59] The morphology control was realized by adding additional reductant, *i.e.* ascorbic acid (AA). In this case, a higher AA concentration leads to the formation of dendritic Pd@Pt core–shell nanoparticles, while the lower amount of AA induces the growth of numerous dendritic branches around the template. When no AA exists, the hollow nanoparticles with porous walls can be prepared (Fig. 6). Zhang and coworkers found that the rate of galvanic replacement between metallic Pd nanocrystals and $PtCl_4^{2-}$ ions was greatly affected by the concentration of Br^- ions and temperature, in which the bromide-induced galvanic replacement reaction had a high selectivity toward the {100} facets of Pd, therefore leading to the formation of cubic Pt–Pd alloy hollow cages[60] or a concave structure[61] when using Pd nanocubes as template. Recently, Xie and coworkers synthesized a series of Rh hollow nanoframes with different types and degrees of porosity by selective chemical etching the Pd cores in Pd–Rh core–shell nanocrystals with distinctive elemental distributions.[62] In addition, some other non-noble metal nanoparticles, such as Ni,[63] Co,[64,65] Cu[66,67] and Al[68] were also used as sacrificial templates to synthesise porous noble metal units. Tellurium or selenium nanowires and nanoparticles were also developed to synthesize uniform 1D Pt, Pd nanowires/nanotubes, platinum nanosponges, nanonetworks, nanodendrites, and Au–Te hybrid nanomaterials on the basis of the galvanic reaction.[69–75]

The porous/hollow silver nanofibers, nanocubes and nanospheres were synthesized by fast reduction of some of the silver salts, such as silver oxide,[76] silver phosphate,[77] silver halides[27] and silver cyanide,[78,79] with BH_4^- or electrochemical reduction. In those reduction reactions, the formation of porous silver structures can be attributed to the occurrence of the Kirkendall effect. For example, Markovich *et al.*[76] prepared hollow silver nanoparticles by the fast chemical reduction of silver oxide nanoparticles. During the reduction process, the Kirkendall effect resulted in solid Ag_2O nanoparticles transforming to hollow Ag nanospheres. Silver orthophosphate has been proved to be a good template to fabricate porous Ag nano/micro units, because it can be easily reduced by reductants, such as AA, $NaBH_4$ and hydrazine. Another advantage for using Ag_3PO_4 as sacrificial template is that the Ag_3PO_4 crystals with well-defined sizes and shapes, such as cubic, octahedral, spherical, wire-like and star-like shapes, have been widely reported,[80–82] and these can be easily accessed and employed in the sacrificial template protocol. Qi and coworkers demonstrated the controlled synthesis of porous Ag microstructures using Ag_3PO_4 as template and AA, hydrazine and $NaBH_4$ as reductant, as shown in Fig. 7.[77] The hollow Ag particles exhibited a well-defined, rhombododecahedral exterior morphology and a remarkably complex hierarchy. In such cases, the final silver structure depended on the inward diffusion rate of the reductant relative to the outward diffusion rate of the Ag^+ ions, namely: single-walled rhombododecahedra formed with AA, due to its lower diffusion rate; double-walled rhombododecahedra formed with hydrazine, which has a medium diffusion rate; and core–shell structured rhombododecahedra formed with $NaBH_4$, which has a higher diffusion rate.[77]

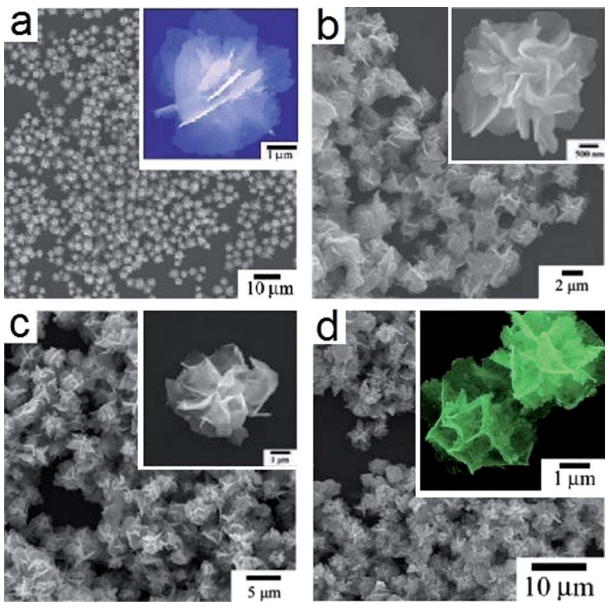

Fig. 5 SEM images of (a) Ag mesoflowers, (b) $Pt_{45}Ag_{55}$, (c) $Pt_{72}Ag_{28}$, (d) Pt mesoflowers. (Adapted with permission from ref. 57, copyright 2012, Elsevier.)

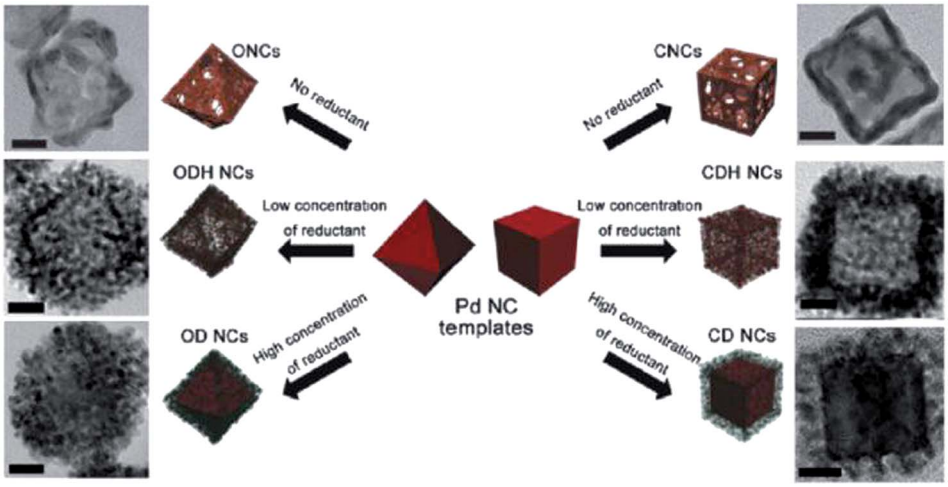

Fig. 6 Schematic illustration for the synthetic parameters to produce various types of PdPt bimetallic NCs from Pd NC templates. Different alloy nanoparticles were synthesized: octahedral nanocages (ONCs); cubic nanocages (CNCs); octahedral dendritic hollow (ODH) NCs; cubic dendritic hollow (CDH) NCs; octahedral dendritic (OD) NCs; and cubic dendritic (CD) NCs. (Adapted with permission from ref. 59, copyright 2012, American Chemical Society.)

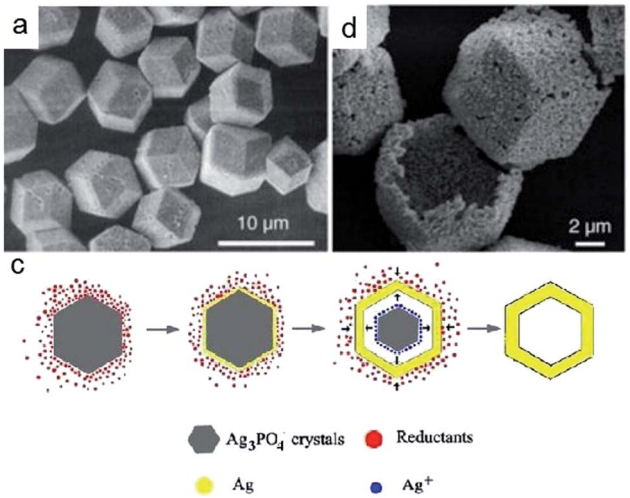

Fig. 7 (a) SEM images of Ag_3PO_4 rhombododecahedral crystals. (b) SEM images of single-walled Ag rhombododecahedral cages after sonication. (c) Schematic illustration of the reaction procedure. (Adapted with permission from ref. 77, copyright 2005, John Wiley and Sons.)

Differently, our previous work showed that when Ag_3PO_4 truncated cubes with a size of around 0.8 μm were used as the sacrificial template and $NaBH_4$ as reductant, porous silver submicrocubes could be obtained rather than core–shell structured particles (Fig. 8).[83] The formation of the pores in silver submicrocubes was due to the volume shrinkage occurring during the reduction of Ag_3PO_4 to Ag. Besides the Kirkendall effect, the formation of porous Ag structures in this case mainly resulted from a volume shrinkage phenomenon occurring in the reduction reaction. During the reduction process the volume of Ag_3PO_4 crystals presented an obvious shrinkage but their morphology did not change. In this case, the fast injection speed and the excessive amount of $NaBH_4$ were the key factors for the formation of porous Ag structures, in which the reduction reaction speed was greatly accelerated, and correspondingly, the size of the as-formed metal nanoparticles decreased with the increase of reduction rate. Then, the generated nanoparticles aggregated together to form porous frames due to the lack of capping agents in solution. The quick formation of extended silver networks preserved the morphology. In addition, the fast reduction of the inner Ag_3PO_4 led to a fast volume collapse of the cubes and prevented the outward flow of Ag_3PO_4, thus causing the formation of a 3-D continuous Ag framework.

The galvanic reaction can also occur between the cuprous oxide and noble metal ionic precursors, thus the methods based on using cuprous oxide as both template and reductant have been proved to be an effective approach to synthesize porous hollow noble metal cages of Ag, Au, Pt, Pd and PtPd alloy.[84,85] Compared to the above widely reported templates, Cu_2O crystals have many obvious advantages, for example, easily controlled

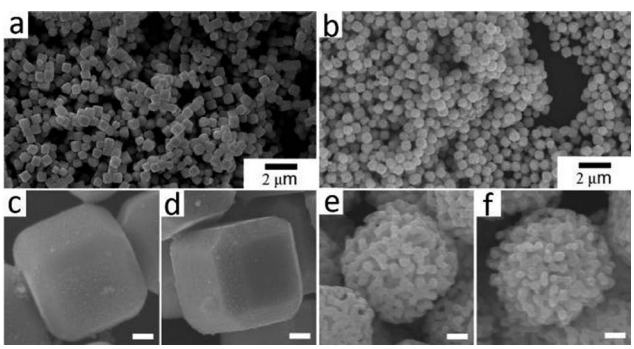

Fig. 8 SEM images of cubic porous Ag submicrocubes (b, e and f) made by using cubic Ag_3PO_4 (a, c and d) as temples. Scale bars are 100 nm. (Aadapted with permission from ref. 83, copyright 2013, the Royal Society of Chemistry.)

structures, cost saving, morphological multiformity, as well as large-scale production.[86] The Cu_2O/Cu redox pair value, −0.36 V, is much lower than that of the noble metal redox pair.[87] Therefore, the ionic noble metal precursors can be reduced to metal.[84,88] Hong and coworkers prepared uniform Pt, PtCu and PtPdCu nanocages with well-defined size and morphology using the correspondingly shaped Cu_2O crystals as sacrificial templates (Fig. 9a–c).[84] Using similar methods, Fang and coworkers synthesized polyhedral gold mesocages with cubic and octahedronal shapes (Fig. 9d and e).[85] Recently, Li *et al.* developed a novel synthesis method for self-supported porous Pt nanostructures comprised of interconnected 2–3 nm Pt nanoparticles by employing the galvanic replacement process between Cu_2O nanocubes and $PtCl_4^{2-}$ ions.[89] In addition, Lee *et al.* reported an electroless Pt deposition on Mn_3O_4 NPs *via* a galvanic replacement process occurring between Mn_3O_4 and $PtCl_4^{2-}$ complexes.[90]

2.1.2 Mesoporous template. The mesoporous materials, such as mesoporous silica, porous anodic alumina membrane and zeolite have been widely used to synthesize 1-dimensional noble metal nanowires.[91] Recently, Wang and coworkers demonstrated a facile approach for the synthesis of uniformly sized mesoporous Pt nanoparticles by using ordered mesoporous silica KIT-6 (Ia3d) and SBA-15 (p6mm) as the hard template and AA as the reducing agent.[92] Typically, the mesoporous silica powders were immersed into an aqueous solution of K_2PtCl_4. After drying the mixture, aqueous AA as a reducing agent was dropped on the powder. The mesoporous Pt nanoparticles were then obtained by removing the silica with HF solution. As shown in Fig. 10, almost all of the obtained meso-Pt nanoparticles presented a rhombic dodecahedral morphology. The meso-Pt corresponds to a perfect inversion replica of the original highly ordered KIT-6 after replacement. The obtained nanoparticles were isolated from each other and had a narrow particle size distribution. The monocrystalline Pt kept the framework structure of the silica KIT-6. Similarly, they also reported well-ordered mesoporous Pt, PtRu PtNi and PtCo nanoparticles with uniform sizes, which were synthesized using mesoporous silica as a hard template.[93–95] The pore size of the porous nanoparticles can be controlled carefully by adjusting the structures of the silica templates. Jaramillo *et al.* successfully fabricated a Pt double gyroid using silica as template.[96] The surfactant and silica can form a double gyroid structure. Calcination at 400 °C can remove the surfactant, leaving a porous structure as the silica template. Through an electrodeposition process, the voids were filled with platinum. After removing the silica gyroid with HF, the double gyroid platinum was formed. In this structure, Pt is in the opposite position of the Si template. Rauber *et al.* reported the direct synthesis of highly ordered large-area Pt nanowire networks with high surface area and excellent transport properties using electrodeposition within the nanochannels of ion track-etched polymer membranes.[97] Takai *et al.* reported a dual template strategy to fabricate the mesoporous Pt nanotubes, in which the formation of mesoporous Pt and Pt-based alloys nanotubes/nanorods was realized through deposition of Pt on lyotropic liquid crystals (LLC), which was coated on the channels of a

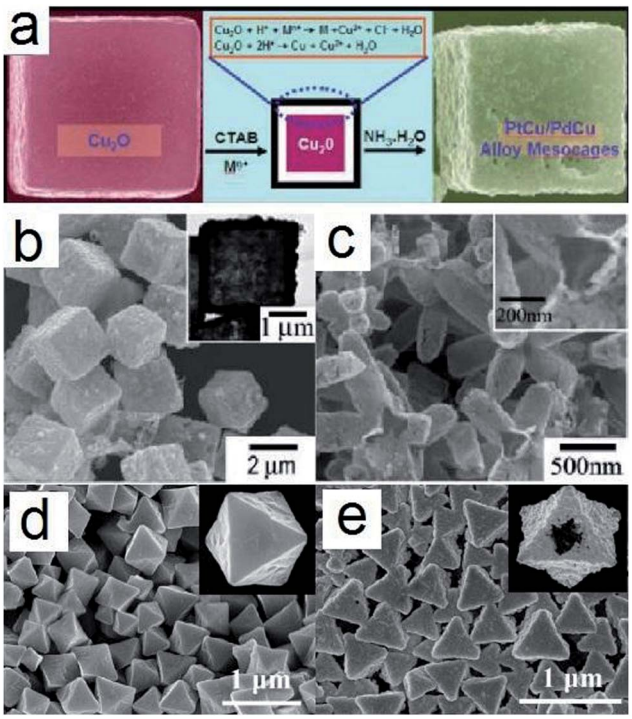

Fig. 9 SEM and images of (b) cubic and (c) star-shaped and hollow PtCu alloy mesoparticles which are obtained by using Cu_2O as template. (adapted with permission from ref. 84, copyright 2011, American Chemical Society). SEM images of octahedrons Au mesocages (e) obtained by using Cu_2O (d) as template. (adapted with permission from ref. 85, copyright 2011, the Royal Society of Chemistry).

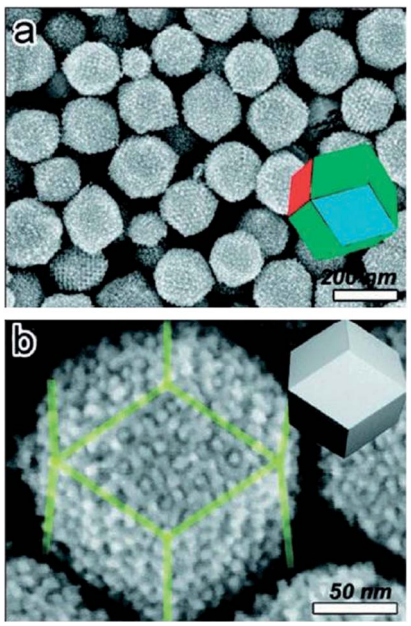

Fig. 10 SEM images of the obtained mesoporous Pt nanoparticles (meso-Pt) prepared with mesoporous silica KIT-6. (Adapted with permission from ref. 92, copyright 2011, American Chemical Society.)

porous anodic alumina membrane surface.[98,99] Morphology control of the final products was realized by external pressure during the coating process.

2.1.3 Copolymer and lyotropic liquid crystals (LLC) template. Compared with the metal oxides including silica and zeolites, the polymeric scaffold has the advantages that the chemical composition, size, morphology and even the penetrability or accessibility of the polymeric scaffold can be tailored.[100] The lyotropic liquid crystal (LLC) phases of surfactants exhibit a rich polymorphism of structures that have long-range periodicities and whose characteristic repeat distances range from 2 to 15 nanometers, which have been utilized as soft templates to synthesize directly mesoporous metals with an hexagonally packed cylindrical mesospace.[101,102] Yamauchi *et al.* demonstrated a synthetic strategy for the preparation of mesoporous Pt particles with giant mesocages connected closely in three dimensions, and the LLCs consisting of diblock copolymers were used as the soft template.[103] By utilizing LLCs physically confined inside the channels of porous anodic alumina membranes, they successfully introduced a stacked donut-like mesospace (circularly packed 1D mesochannels) into the Pt fibers.[104] A porous Ag nanowire can be fabricated by using poly(styrene-*alt*-maleic anhydride) as template.[78] Porous gold nanobelts consisting of self-organized nanoparticles were synthesized by a morphology-preserved transformation from metal–surfactant complex precursor nanobelts formed by surfactant and $HAuCl_4$.[105] Pan and coworkers prepared a two dimensional (2D) and 3-D porous dendritic Au nanostructure through a seeded growth assisted by in-situ polymerized polyaniline.[106,107] On the basis of an random amphiphilic copolymer poly(methacrylic acid 2-(diethylamino) ethyl ester-*co*-octadecyl, poly(ethylene glycol)-butenedioate) (P(DEAEMA-*co*-O-B-EG)) used as the template, Yuan and coworkers prepared porous 3-dimensional (3-D) Au nanostructures with controllable morphology and high yield *via* the direct reduction of hydrochloroauric acid ($HAuCl_4$) by AA, as shown in Fig. 11.[108] The morphology of the final products was simply controlled by changing the PEG molecular weight from 400 to 600 in P(DEAEMA-*co*-O-B-EG). Interestingly, these porous 3D Au nanostructures are composed of radially arranged thin nanosheets rather than the nanowires and nanoparticles which endow them with a well-defined 3D structure. Robinson and coworkers prepared nanoporous palladium and platinum powders with a particle diameter around 50 nm and a pore size of 3 nm on the milligram to gram scales by chemical reduction of tetrachloro complexes by ascorbate in a concentrated aqueous surfactant at temperatures between −20 and 30 °C.[109] The assembly of high concentration of the surfactant Brij 56 into hexagonally packed cylinders offers a template to confine the reduction and growth of metal particles into zeolite-like mesoporous structures.

2.1.4 Surfactant micelle and bicelle template. Shelnutt's group developed a series of synthetic methods for the preparation of porous Pt nanodendrites, nanowheels, nanosheets, nanocages and hollow nanospheres using surfactant micelles (liposomes) and bicelles as growing templates.[110–118] Those methods were based on a seeding and fast autocatalytic growth approach. The ionic platinum precursor was reduced by AA or porphyrin photocatalyst (hydrophobic tin(IV) octaethylporphyrin, SnOEP) irradiated by visible light in the presence of surfactant-formed liposomes or bicelles. The formation of such complex nanostructures was due to the inhomogeneous nucleation of Pt seeds at the surface or interface of the micelles or bicelles. A typical example is shown in Fig. 12, and the dendritic character of the constituent nanosheets make the

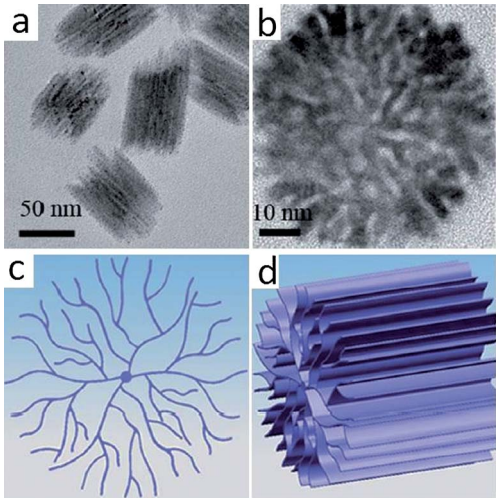

Fig. 11 Three-dimensional gold nanodendrimers: using polymer as template. (Adapted with permission from ref. 108, copyright 2012, the Royal Society of Chemistry.)

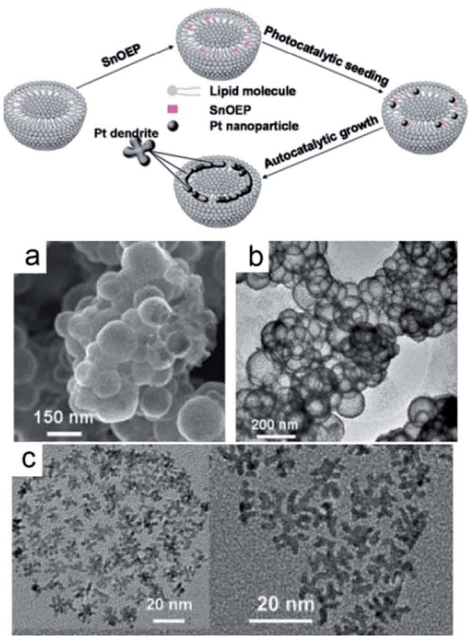

Fig. 12 Diagram of steps in the synthesis of spherical platinum nanocages. (a) SEM images of hollow platinum nanocages; (b) hollow platinum nanocages (adapted with permission from ref. 112, copyright 2006, John Wiley and Sons); (c) TEM images of platinum nanoparticles grown on 140 nm liposomes prepared in water. (Adapted with permission from ref. 111, copyright 2006, American Chemical Society.)

hollow spheres highly porous. The unilamellar liposomes containing hydrophobic SnOEP in the liposomal bilayer were prepared by a process of solvent evaporation, hydration, and extrusion. Using white light to reduce photocatalytically Pt complexes produces metal seed particles upon irradiation of the liposomes containing the SnOEP.[112] The Pt nanoparticles formed in the reduction reaction and they provided seeds for the growth of dendritic Pt nanosheets. When the seed particles reach a certain size they begin to form dendritic nanosheets. The dendritic growth continues until the Pt complex is exhausted, thus the size of the Pt dendrites is determined by the total Pt complex available and the number of seeds produced. Stucky's group reported an efficient approach to produce thin platinum meso-porous films (~50 nm) through an electrodeposition process.[119] In such a case, the surfactants (*e.g.* sodium dodecyl sulfate, SDS) could be assembled electrochemically into a micelle film at the solid–liquid interface, which acted as a soft template to form a porous Pt nanofilm. Recently, Yamauchi's group developed Stucky's approach. They found that the pore sizes of the as-prepared porous Pt nanofilms can be well controlled by using different kinds of surfactant.[120] In a similar way, Pt based meso-porous alloy films, such as PtCu and PtRu, were also prepared and reported.[121,122] In addition, when the electrochemically controlled assembly of surfactants and deposition of platinum were performed in the nanochannels (*e.g.* porous polycarbonate, PC, membrane), one-dimensional mesoporous Pt nanorods can be prepared.[123] Furthermore, the non-ionic surfactant, Pluronic F127, was found to self-assemble on the surface of colloidal silica particles to form micelles without the help of an electrochemically driven approach. By using this novel core–shell structure as a soft@hard template, they synthesized mesoporous Pt–Ru particles with a hollow interior and tunable shell thickness.[124]

2.1.5 Etching/corrosion method. An etching/corrosion procedure can be used to remove selectively certain facets from the nanocrystals and the less stable elements from alloys, thus producing a porous structure. Furthermore, tuning of the etchant strength and reaction conditions allows precise control of the morphology and porosity of the final products.[21,125,126] Series of enchants have been developed to synthesize the porous noble metal nanostructures, typically including Fe^{3+}, HNO_3/NO_3^-, O_2, I^-, H_2O_2 and so on (Table 1). Typical examples are the synthesis of porous noble metal nanostructures through etching off the Ag using Fe^{3+} ions and HNO_3 from the AgPt[49,127] and AuAg[128–130] alloys, which were prepared through a galvanic reaction between the Ag sacrificial template and the Pt or Au ionic precursors. By removing the residual silver with HNO_3, Alia and coworkers prepared porous platinum nanotubes (PtNTs) with a thickness of 5 nm, an outer diameter of 60 nm, and a length of 5–20 μm by galvanic displacement with silver nanowires.[49] Chen *et al.* synthesized the hollow Pt nanosphere catalysts with nanochannels at room temperature with silver nanoparticles as a sacrificial template. After removing the Ag from the PtAg alloy formed during the galvanic reaction, the nanochannels and voids were produced on the surface of the hollows.[127] Similarly, H_2O_2 and Fe^{3+} was also used to etch off selectively Ag from the AgAu bimetallic nanoparticles to produce porous Au frames (Fig. 13).[128] Xiong *et al.* synthesized

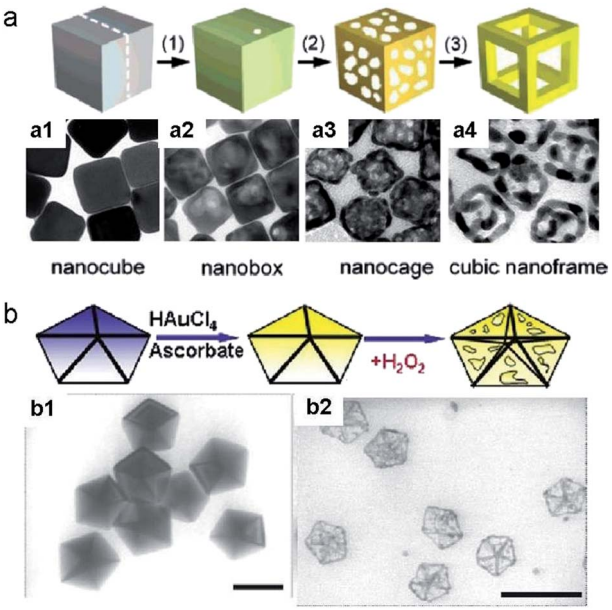

Fig. 13 (a), The schematic drawing and TEM images of the formation of an Au cubic frame: (a_1) 50 nm Ag nanocubes; (a_2) Au–Ag alloy nanoboxes obtained by reacting the nanocubes with 4.0 mL of 0.2 mM $HAuCl_4$ aqueous solution; (a_3 and a_4) nanocages and nanoframes obtained by etching the nanoboxes with 10 and 20 μL of 50 mM aqueous $Fe(NO_3)_3$ solution. (Adapted with permission from ref. 128, copyright 2007, American Chemical Society.) (b) Illustrating the formation of gold nanoframes and nanocages upon deposition of gold onto decahedral AgNPs and subsequent silver dissolution with hydrogen peroxide: (b_1) silver decahedra prior to gold deposition; (b_2) decahedra after deposition of gold; (b_3 and b_4) images of the frames and cages after dissolution of silver with different amount of hydrogen peroxide. (Adapted with permission from ref. 146, copyright 2011, American Chemical Society.)

Table 1 Summary of the etchants applied in the synthesis of porous noble metal units

Etchants	Targets	Shape of the products	Ref.
$Fe(NO_3)_3/FeCl_3$	AgAu alloy, Pd	Cubic nanoframe, corolla-like Pd NPs	128 and 129
H_2O_2	Ag	Porous nanoshell	133
KI	Au	Nanocages	132
HNO_3	AgPt, AuAg alloys, Pd–Ni	Porous hollow Pt shells,Au and Pd NPs	49, 57, 117, 130 and 134
O_2	Pd	Pd cubic cages, porous single-crystalline Pd NPs	19 and 131
Electrochemistry	Pt-on-Ag, Pt–Cu, Pt–Co	Porous hollow Pt or Pt-M spheres/cubes	135–138

single-crystal Pd nanoboxes and nanocages by an O_2 induced corrosion pitting process.[131] In such a process, the combination of continuous etching of the Pd nanocube from the interior and some reduction of the Pd(II) species at the edge of the hole leads to the formation of a Pd nanobox. Fan and coworkers presented a strategy to achieve cage- and ring-like Pt nanostructures through a heterogeneous seeded growth of Pt on Au nanocrystal surfaces followed by selectively etching off the Au seeds with *in situ* formed I_2.[132] Recently, Wang and coworkers reported a facile method for the preparation of porous single-crystalline Pd NPs with controllable sizes.[19] They considered that the rapid growth of the crystals induced many small crevices on the initially formed Pd NPs. Then, oxidative etching occurs preferentially at the highly active sites in the crevices owing to the presence of Cl^- and O_2 in the solution, giving the porous structure. Besides adding the oxidants, electrochemically etching-off the less stable species from the alloy NPs was proved to be an efficient approach to produce the porous nanostructures. Yang's group produced porous hollow Pt nanospheres and cubes by electrochemically removing the Ag species from Pt-on-Ag Pt bimetallic nanoparticles.[135,136] After treatment under various potential cycling profiles, Pt cubic nanoboxes with an average edge length of about 6 nm and a wall thickness of 1.5 nm were synthesized. The reduction reaction kinetics of the metal precursors can be well controlled by introducing the etchant into the reaction.[139–141] Huang and coworkers demonstrated an etching-assisted method to prepare corolla-like Pd mesocrystals consisting of unidirectionally aligned, well-spaced, and connected ultrathin (1.8 nm-thick) Pd nanosheets, as shown in Fig. 14.[129] In the synthesis process, CO acts as the surface-confining agent to allow anisotropic growth of Pd nanosheets as branches, while Fe^{3+} etches the Pd seeds at the early stage of the reaction to induce formation of the branched structure.

2.1.6 Overgrowth synthesis. Controlled overgrowth of concave cubic seeds can induce a hollow octahedral structure. Langille *et al.* synthesized Au octahedra with hollow features through the controlled overgrowth of preformed concave cube seeds.[142] The overgrowth of the concave Au nanocubes was attributed to that the underpotential deposition (UPD) of Ag species occurred selectively on their {111} facets, leading to the stabilization of these crystal planes in the presence of a relatively higher Ag^+ concentration. As shown in Fig. 15, the UPD process caused the formation of small {111}- faceted "plates" at the eight tips. Then the size of the plates increased and the tips of an octahedron would form when the plates met together. (Fig. 15) DeSantis *et al.*[143] demonstrated an overgrowth processes for the preparation of bimetallic Au–Pd octopods and concave alloy nanostructures including hopper-like nanocrystals with deep angular concavities through seed- mediated co-reduction of two metal precursors. Similarly, the presence of seeds that serve as preferential sites for the growth of the larger nanostructures and the preferential growth of certain facets lead to the formation of such novel Au–Pd bimetallic structures. On the other hand, to manipulate carefully the growth kinetics by introducing some additives, such as Br^- and Cl^- ions, to slow the precursor reduction was a critical procedure to favor metal deposition on the highest energy features.[61,144,145]

2.2 Colloidal synthesis

The term 'colloid' refers to a two-phase system where insoluble particles are dispersed in water or, broadly speaking, in

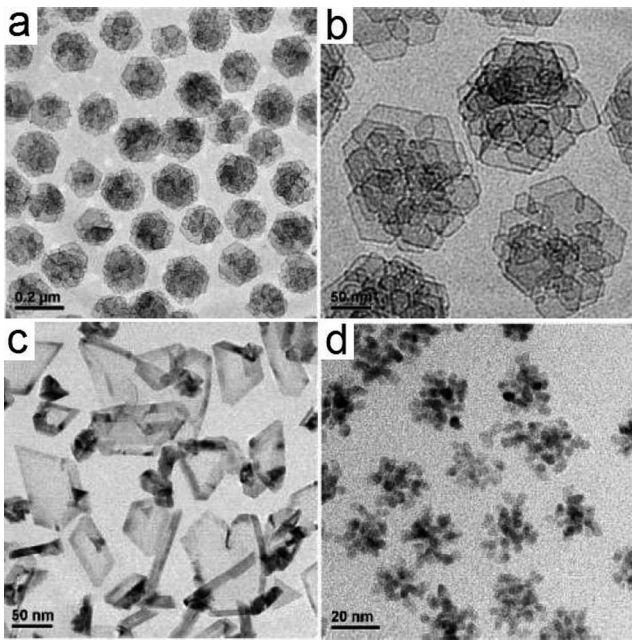

Fig. 14 (a and b) TEM, HRTEM, images of corolla-like Pd mesocrystals. Pd nanocrystals prepared under reaction conditions in the absence of $FeCl_3$ (c) and in the absence of CO (d). (Adapted with permission from ref. 129, copyright 2011 American Chemical Society.)

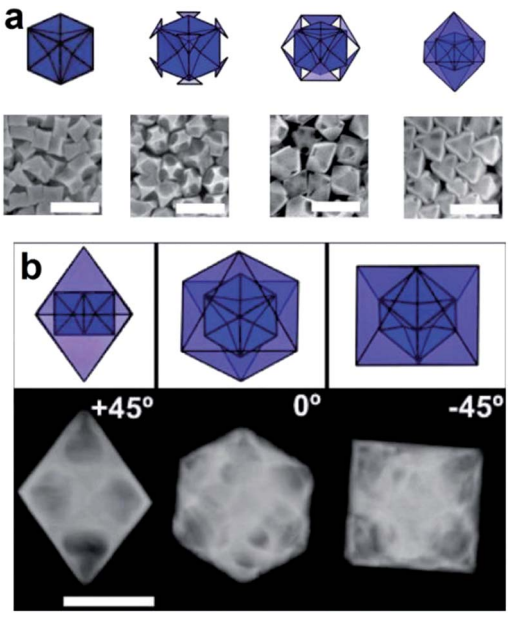

Fig. 15 (a) The schematic and SEM images of concave cube seeds and the products of the octahedra reaction with different amounts of $HAuCl_4$ solution. (b) The model and STEM images of a single hollow octahedron at different orientations. Scale bars: 100 nm. (Adapted with permission from ref. 142, copyright 2011, American Chemical Society.)

solvents.[147,148] The preparation of porous noble metal NPs with designed sizes through a colloidal approach has been found to be effective. Compared to the template method, which involves the tedious synthetic procedures of multiple steps, the colloidal synthesis is more like a "one-pot" process which can provide a facile route for a large-scale synthesis. However, how to control precisely the porosity and morphology in the colloidal solution still remains a challenge for nanosynthesis. The reduction of ionic noble metal precursors by reducing agents in the presence of capping agents is a general method for preparing noble metal nanoparticles in colloidal solutions. As for the porous noble metal nanoparticles, the nucleation and growth process of the crystals needs to be controlled carefully to avoid forming solid nanoparticles. Generally, the formation of the pores in the nanoparticle growth needs dendritic growth behavior or aggregation of isolated crystals through a random or oriented attachment (OA) process.

2.2.1 Dendritic growth. The dendritic growth of noble metal nanocrystals was considered to depend greatly on the number and type of twin planes in the initially formed seed crystals. These stacking faults would break the symmetry in face-centered cubic metals, such as platinum, and enable the formation of anisotropic metal nanocrystals with 1-D, 2-D and 3-D morphologies, which has been widely reviewed by many research groups.[25,31,149–157] Therefore, only a few typical examples for the formation of multipods and porous structures are selected and presented here. Fig. 16 shows typical examples in which multi-branched nanostructures grow from seeds with a single crystal cuboctahedron. Besides altering the seed structures, surfactant molecules can sometimes adsorb selectively on certain facets of the NPs, which prevents the metal atoms depositing on these crystal planes, thus inducing the dendritic/anisotropic growth of noble metal NPs.[29] An example is the synthesis of Pt multipods from H_2PtCl_6 in the presence of oleylamine and cetyltrimethylammonium bromide (CTAB). In this approach, oleylamine (OA) is considered to act as a ligand to form stable Pt^{4+} complexes and lead to the reduction of Pt^{4+} complexes to a metallic state at an elevated temperature. Cetyltrimethylammonium bromide (CTAB) plays the role of a structure-directing agent to induce the growth of Pt nanocrystals along the {111} direction and thereafter the formation of hierarchical nanoassemblies, as shown in Fig. 16d and e.[158] In addition, the growth of the noble metal nanoparticles was generally ascribed to a kinetically controlled mechanism based on slow, continuous nucleation (seeding) and fast autocatalytic growth.[110,159] Thus, the overgrowth which occurred during the self-catalysis process was often used to deduce the formation mechanism of branched nanostructures.[160,161] The porous Pt or Pd nanodendrites have been produced in aqueous solution simply by reducing an aqueous solution containing an ionic Pt or Pd precursor and formic acid or AA in the presence of surfactant molecules without the need for any template and seed mediated growth.[162–165] The growth of Pt dendrites in the presence of nonionic surfactants, such as Brij 700, Tetronic 1107, PVP and PVP-*co*-VA, (Fig. 17) was ascribed to the point that their functional groups can anchor onto the deposited platinum surface, leading to a continuous growth/termination process of the porous Pt nanodendrites, in which the branch terminal served as a new nucleation site, inducing the continuous growth of the new branches until the depletion of the precursor, as described by Zhang *et al.*[166]

Besides the pure noble metal porous NPs, a series of porous/dendritic bi- and poly-metalic nanoparticles with A-on-B,[167–174] core–shell[175–179] and alloy[60,180–190] structures have been widely reported. A typical example is the synthesis of unique Au@Pd@Pt triple-layered core–shell structured nanoparticles consisting of an Au core, a Pd inner layer, and a nanoporous Pt outer shell, which was reported by Wang and coworkers.[169] The

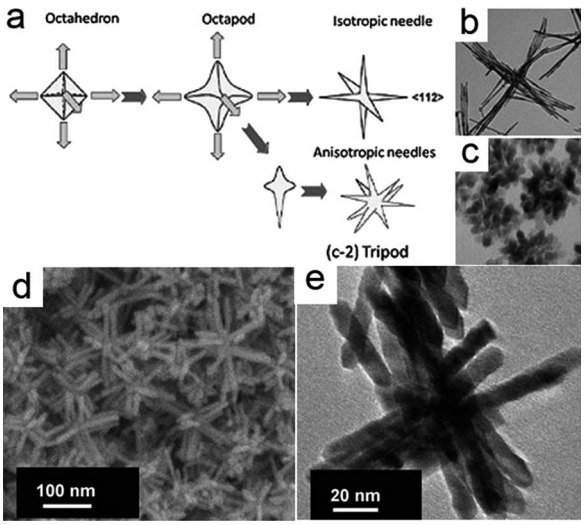

Fig. 16 (a) Possible formation mechanisms of branched nanostructures from seed crystals (adapted with permission from ref. 152, copyright 2010 Wiley-VCH); the octahedral nanocrystals evolving into (b) isotropic needles or (c) anisotropic nanostructures from the tips of the seeds (adapted with permission from ref. 29, copyright 2013 the Royal Society of Chemistry). (d) and (e) TEM and SEM image of the branched nanoparticles (adapted with permission from ref. 158, copyright 2012, Wiley-VCH).

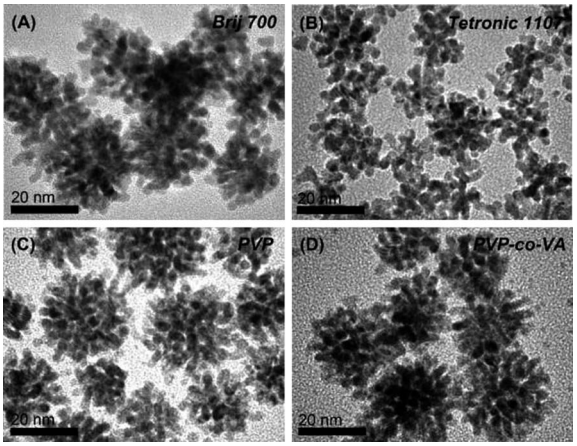

Fig. 17 Platinum nanostructures prepared with different nonionic organic molecules: (A) Brij 700, (B) Tetronic 1107, (C) PVP, and (D) PVP-*co*-VA, respectively. (Adapted with permission from ref. 162, copyright 2010, American Chemical Society.)

growth of such a novel structure was attributed to an auto-programmed process, in which the initially formed Au nanoparticles served as *in situ* seeds for subsequent depositions of the Pd inner layer and porous Pt outer shell. The capping agent, *i.e.* Pluronic F127, served as a structure-directing agent to direct the nanodendritic Pt outer shell growth. Through a similar approach, this group prepared novel mesoporous Pt on Pd core–shell nanoparticles with a concave structure. The whole particle presented single crystal character, which was attributed to the epitaxial growth of the porous platinum shell from the palladium seed.[191]

2.2.2 Nanoparticle aggregation. The aggregation of the pre-grown nanocrystals through a random or regular form is likely to cause the formation of pores in the final nanostructures. As shown by the schematic drawing in Fig. 18, the random aggregation of the crystals can be explained by the sintering which occurs between the attached nanocrystals even though they have no consistent crystallographic orientation, thus favouring the formation of porous nanoparticles with a polycrystalline structure. As for the regular aggregation form, it can be ascribed to a nonclassical crystal growth model, *i.e.* the oriented attachment (OA) model, in which the basic growth units are NPs, rather than atoms/ions in the classical growth. In the OA dominated growth model, the nanocrystals align along a common crystallographic direction in order to minimize their interface energy.[192] This particle-mediated growth model often leads to the formation of so-called mesocrystals, an ordered superstructures composed of many individual nanocrystals that share common crystallographic planes, exhibiting crystal structures similar to those of single crystals.[29,193,194]

As shown in Fig. 19, Wang and coworkers developed a non-capping-agent strategy to prepare porous dendritic platinum nanoparticles just by heating a mixture of an aqueous solution of chloroplatinic acid (H_2PtCl_6), sodium hydroxide (NaOH) and AA.[195] Since no capping agents existed in the solution, the growth and aggregation of the nanocrystals showed a large random character. As shown clearly in the TEM images of the intermediate products at different time intervals, the growth of the final porous nanodendrites is based on the step-by-step attachment of the as-formed nanocrystals. The corresponding selected-area electron diffraction (SAED) pattern indicates that the structure of the single particle is polycrystalline. Similar

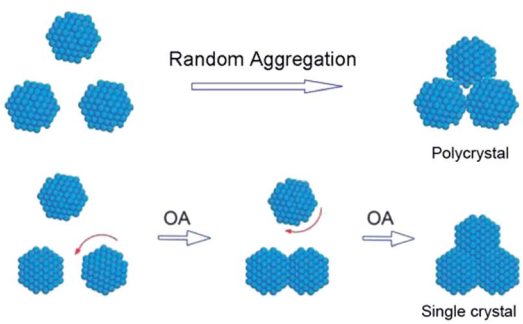

Fig. 18 Illustration of particle-mediated growth. (Adapted with permission from ref. 29, copyright 2013, the Royal Society of Chemistry.)

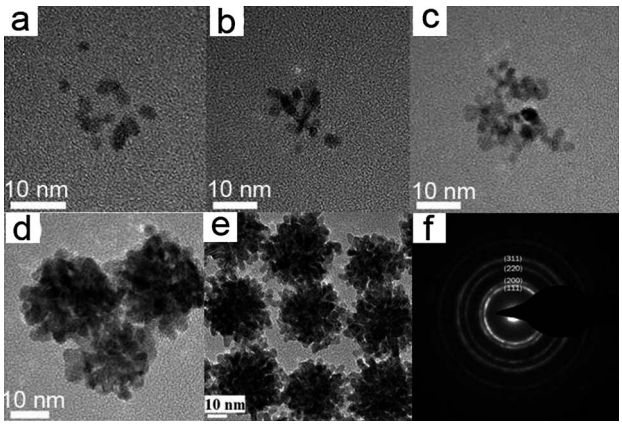

Fig. 19 Pt nanodendrites synthesized without using organic solvents or surfactants. (a–d) TEM images of the intermediate products sampled at different reaction times: (a) 4, (b) 5, (c) 6, (d) 8 min. (Adapted with permission from ref. 195. Copyright 2012, the Royal Society of Chemistry.)

growth behavior was also found in the sonication-assisted reduction of Pd precursors in aqueous solution with AA or hydrazine hydrate to produce porous Pd nanodendrites without any capping agents.[196,197] Viswanath *et al.* reported that porous nanosized Pt aggregates with a specific surface area of 39 $m^2\ g^{-1}$ were synthesized by tuning the electrostatic interaction between surfactant-free nanoparticles in the solution phase, without using any capping agents.[198] Porous Pd black with a high electrochemical active surface area of about 40.2 $m^2\ g^{-1}$ was synthesized through a heterogeneous catalytic reaction of formic acid decomposition.[199] In addition, some other groups found that even in the presence of capping agent, such as PVP, CTA^+ and nonionic block copolymers, the reduction of ionic Pt precursors through reducing agents, sonoelectrochemical or sonicating treatment would lead to the formation of Pt nanodendrites or nanosponges by assembling the initially produced NPs.[200–203] Chen and coworkers prepared porous Pd and Pt–Pd alloy nanospheres using the polyallylamine hydrochloride (PAH) as complexing agents under mild reaction conditions, and the particle size of the porous nanospheres could be controlled readily by altering the ratio of noble metal precursors to PAH.[204,205] The formation of the porous nanospheres was ascribed to the attachment between the primary nanoparticles.

The oriented attachment is a classical formation mechanism suggested to explain the formation of complex nanostructures based on particle-mediated growth, such as mesocrystals. As building units, the NPs prefer to attach to each other through the facets with highest surface energy or surface area in order to decrease the total free energy. Thus the shape and structure of the primary building units needs to be well controlled. For example, as shown in Fig. 20f–h, during the formation of 3-D PtRu alloy porous mesocrystals, the primary NPs showed a truncated octahedral shape (Stage 1), in which, the {111} facets have a larger area than the {100} facets and they were less protected than the {100} faces. In addition, the secondary growth occurred preferentially at the {111} facets (Stage 2). Therefore, this oriented attachment growth model ultimately

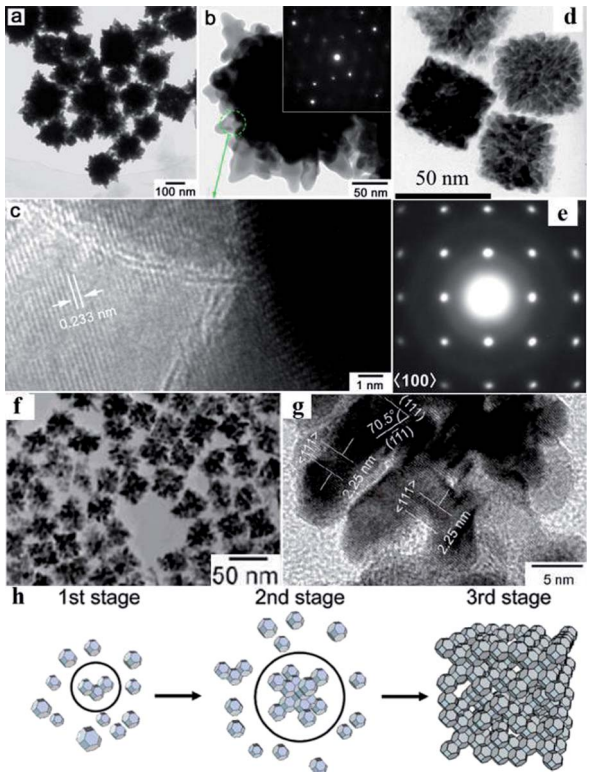

Fig. 20 The TEM images of Au (a–c) (adapted with permission from ref. 207, copyright 2012, the Royal Society of Chemistry), Pt (d–e) (adapted with permission from ref. 208, copyright 2010, American Chemical Society.) and PtRu alloy (f–g) (adapted with permission from ref. 206, copyright 2007, American Chemical Society.) mesocrystalline NPs with porous structures. The corresponding HRTEM images and SAED patterns indicating the single crystal characters of the corresponding NPs. (h) Illustration of the formation of 3D PtRu mesocrystals. (adapted with permission from ref. 206, copyright 2007, American Chemical Society.)

leads to the formation of dendritic nanostructures with well-defined morphology and single crystalline character. (Stage 3).[206] Many strategies for the synthesis of porous noble metal mesocrystal NPs have been developed. Our group prepared gold mesoparticles with various morphologies and highly roughened surfaces, including sea urchin-like (Fig. 20a), flower-like, star-like, meatball-like, and dendritic nanostructures using a pentanol/water interface as a growth ''bed''.[207] Nogami *et al.* reported single-crystalline platinum nanocubes with porous morphology by using ethylene glycol, HCl and polyvinylpyrrolidone as the reducing agents of H_2PtCl_6, as shown in Fig. 20d.[208] Similar platinum nanostructures were prepared through decomposing platinum acetylacetonate ($Pt(acac)_2$) in a hot diphenyl ether (DPE) solution in the presence of 1,2-hexadecanediol (HDD), hexadecylamine (HDA) and 1-adamantanecarboxylic acid (ACA).[18] Xia's group synthesized highly faceted Pt nanocrystals with porous structures by reducing a H_2PtCl_6 precursor with PVP in an aqueous solution containing a trace amount of Fe^{3+} ions.[209] Huang *et al.* demonstrated an etching assisted approach to synthesize corolla-like Pd mesocrystals consisting of unidirectionally aligned, well-spaced and connected ultrathin (1.8 nm thick) Pd nanosheets.[129]

Besides the 3-D mesocrystals, the OA process can also induce the formation of 1-D nanowires[210] and 2-D porous single crystal sheets,[110] nanonetworks and nanoplates.[211–213] Xu and coworkers prepared 2-D dendritic platinum circular nanosheets with single crystal and porous character by means of liposomes as template.[110] Our previous work showed that the continuous UV irradiation of the primary Au NPs using citric acid as a reducer and protective agent led to transformation of the NPs into 2-D nanonetworks; porous nanoplates with hexagonal, triangular or truncated triangular pores.[211–213] The formation of such porous 2-D Au nanostructures was due to the oriented attachment and fusion of the initially produced NPs.

3. Applications of porous noble metal units

The production of particulate materials with high porosity, defined shapes and monodispersed sizes would increase further the spectrum of applications of noble metal NPs. This is because the ratio of external to internal atoms of the porous colloidal noble metal NPs increases rapidly as the particle size decreases compared to their solid counterparts, leading to the NPs possessing a higher specific surface area and surface activity. In addition, smaller particle sizes have reduced the diffusion path lengths relative to conventional bulk porous noble metal materials. Therefore, the improved properties of the porous noble metal units afford many potential opportunities for their application in catalysis, drug delivery, cell imaging and SERS.

3.1 Medical applications

3.1.1 Drug delivery. To develop novel nanocarriers loaded with anticancer drugs to improve therapeutic efficiency and avoid side effects has been considered a new breakthrough in cancer targeting and treatment.[214,215] There are three basic properties necessary for the candidate materials as drug delivery carriers: lower systemic toxicity; a suitably sized carrier; and controlled release of the loaded drugs.[216,217] Over the past decades, gold NPs with various structural features have became one of the most widely studied materials as drug delivery carriers due to their higher chemical stability, lower cytotoxicity, biocompatibility and structural diversity at the nanosize. In addition, gold NPs with special morphologies displayed a strong surface heat flux upon absorption of NIR light, thus they were selected as an excellent candidate for NIR light-triggered photothermal ablation (PTA) therapy and release of a drug from nanocarriers, as well as a photothermal treatment agent.[215,217,218] Based on their unique structure features, porous gold NPs were very suitable for applications in drug delivery,[14,16,219,220] owing to their higher drug loading amount and controllable release. The generally used porous gold NPs were gold nanocages and gold nanoshell nanomicelles.

Gold nanocages can be synthesized through the galvanic replacement reaction, which is required for good uniformity in terms of both size and shape, as this will affect their optical properties and alter their biodistribution.[221] Availability in large

quantities was also required for *in vivo* studies. As a result, one needs to produce Ag nanocubes with uniform, controllable sizes and quantities on the scale of grams per batch. For both diagnostic and therapeutic applications, it is critical to deliver Au nanocages exclusively to the malignant site. In addition, it is necessary to engineer the size, shape, and surface properties of Au nanocages to optimize their targeting by the desired biological system.[13,215]

The gold nanoshell nanomicelles were generally prepared through a cross-linked molecular-assisted assembly of gold nanoparticles.[214,217,218,222–224] As shown in Fig. 21, Niikura and coworkers demonstrated a synthetic approach for the preparation of Au hollow NP assemblies (NP vesicles) by cross-linking each gold nanoparticle with thiol-terminated PEG.[223] The water soluble AuNVs can be used as a drug delivery carrier enabling light-triggered release. The pores on the surface of AuNVs can be controlled by heating temperature: at a higher temperature, *i.e.* 62.5 °C, the stretch of the linker molecular would lead to gaps between the openings of the nanoparticles, which is conducive to drug loading; while the drug or dye can be encapsulated inside the vesicles due to the closure of these gaps at room temperature, the heating of the AuNVs by short-term laser irradiation (5 min, 532 nm) leads to the gaps opening again and releases the encapsulated drug or dye.[223]

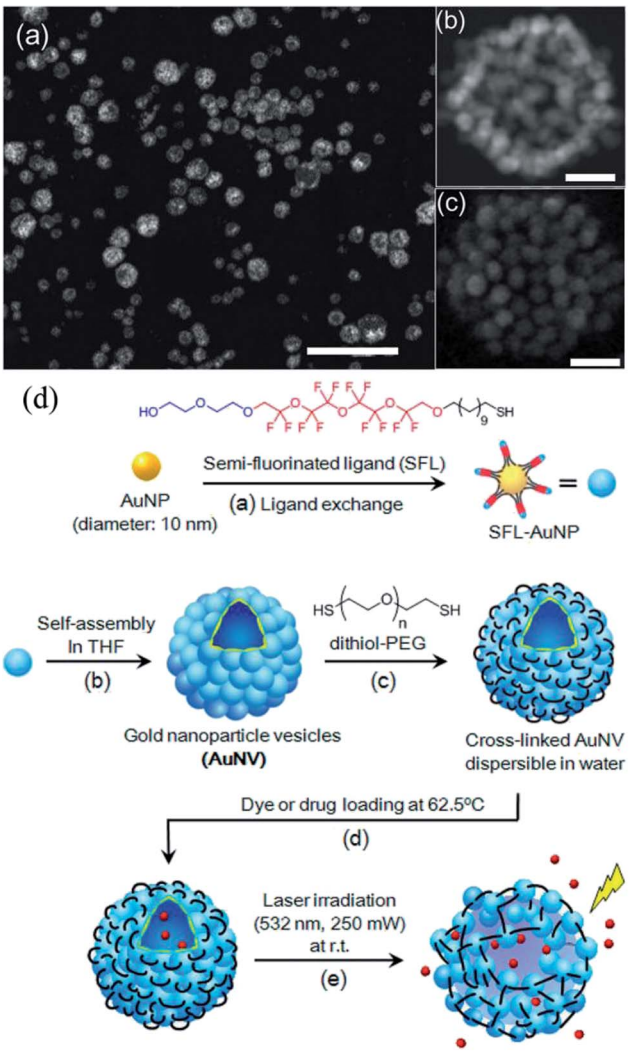

Fig. 21 (a) STEM image of AuNVs cross-linked with dithiol-PEG (M_n = 3400) cast from water. (b) STEM and (C) SEM images of a single crosslinked AuNV. The scale bars are (a) 400 and (b and c) 20 nm. (d) The schematic drawing for the fabrication of gold NP vesicles (AuNVs) encapsulating dye or drug molecules and their light-triggered release. (Adapted with permission from ref. 223, copyright 2013, American Chemical Society.)

3.1.2 Cell imaging. The high scattering optical cross section and photothermal properties of the Au nanocages or nanoshells make them potentially valuable contrast agents for photonics-based imaging modalities,[225] mainly including optical coherence tomography (OCT) and photoacoustic tomography (PAT). The OCT imaging is based on contrast from spatial variations in tissue scattering.[226,227] By introducing the NIR resonant Au nanocages as contrast agents, Zhou and coworkers realized the *ex-vivo* imaging of human breast tissue using the photothermal OCT imaging technique.[226] The PAT technique was based on the detection of the spatial variation in the optical absorption of tissues which could be enhanced greatly through use of NIR photothermal contrast agents,[32,228] thus providing good ultrasonic spatial resolution, because the PA imaging modality was very sensitive to endogenous and exogenous optical contrasts.[229] Wang's group demonstrated the feasibility of using Au nanoshells grown on silica particles as contrast-enhancing agents for PAT.[228] The existence of PEG coated nanocages circulating in the vasculature of a rat brain greatly enhanced the optical absorption in the brain vessels by up to 63% after three sequential administrations of nanoshells. In addition, the porous gold nanospheres have been used to image and compare the live and dead cells. Shukla and coworkers estimated the cell-staining effect of porous Au NPs and solid Au NPs by binding of a fluorescent molecule, propidium iodide (PI).[17] PI is a standard fluorophore used to distinguish between live and dead cells. The cells stained with PI–porous nanogold conjugates show a significantly enhanced fluorescence compared to cells stained with PI–solid gold conjugates. This was attributed to the enhanced surface area of the porous gold nanospheres for binding of the fluorescent dye, thus improving the fluorescence in cell-staining.[17]

3.2 SERS substrates

Noble metals, especially Ag and Au are promising materials to fabricate SERS-active substrates with high performance for Raman enhancement.[160,230,231] Besides their size and shape, the surface topography is significant as an enhancement factor. The porous structures usually have rough surfaces due to their porous features, which leads to them having a relatively high performance in SERS.[22,83,207,232–248] The rough surface often provides gaps and protuberances which can generate "hot spots" and enhance the Raman scattering strongly due to local electromagnetic field enhancements. Fig. 22 shows that the Au mesocrystals exhibit the highest SERS enhancement, on the order of $\sim 10^7$–10^8, compared with the dendritic and polyhedral Au particles. This high performance is due to the Au

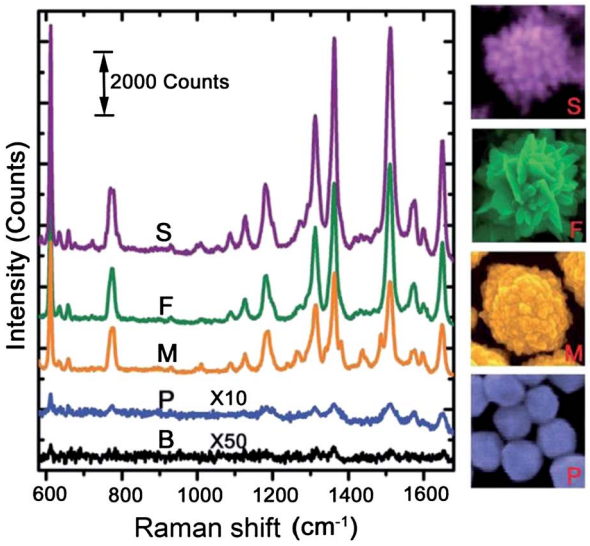

Fig. 22 SERS spectrum of R-6G adsorbed on the surface of the substrates composed of different gold mesoparticle films: S: sea urchin-like, F: flower-like, M: meatball-like, and P: polyhedral. B indicates 'background'. (Adapted with permission from ref. 207, copyright 2012, the Royal Society of Chemistry.)

mesocrystal having a rough surface and high internal porosity.[207] Yang and coworkers reported a bacteria-templated synthesis of silver microspheres with hollow and porous structures.[249] The SERS experiments using 2-mercaptopyridine (2-Mpy) as probe molecules showed that the hollow porous microspheres presented an ultrasensitive molecular detection performance. The detection limit was as low as 10^{-15} M and the enhancement factor reached 10^{11}.

3.3 Fuel cell catalysts

In recent years, the increase in global energy requirements and environmental awareness, as well as the perceptible shortage of raw materials, has put forward public requirements for the development of clean, efficient energy conversion techniques.[250] Proton-exchange membrane fuel cells (PEMFCs) are showing great promise as an alternative to environmentally unfriendly use of fossil fuel. Pt, Pd and their alloy-based catalysts are the best choice for the electrochemical oxidation of small organic molecules (*e.g.*, methanol, ethanol, formic acid) as well as for oxygen reduction reactions, which are critical electrode reactions in fuel cells.[19,57,66,151,153,196,251–277] The catalytic activity of those noble metal catalysts can be closely related to their structure, composition and shape,[278,279] because most electrocatalytic reactions are sensitive to the electronic structure and the crystalline surface structure, which can be controlled by their composition and shape, respectively.[158,280–283] Porous Pt, Pd and their alloy-based nanoparticles possess the characteristics of high surface area, low specific density, good mass conductivity and rich surface chemistry, thus they have become one of the most frequently studied materials for application in PEMFC catalysts. For example, Zhang and co-workers[44] found that the porous Pt dendritic nanotubes synthesized through the galvanic replacement reaction between Ag dendrites and H_2PtCl_6 presented 2.33-fold greater activity on the basis of equivalent Pt mass, 4.4-fold more activity in terms of specific activity for ORR than the state-of-the-art Pt/C commercial catalyst, 5.25-fold more activity on the basis of equivalent Pt mass and 3.68-fold more activity in terms of their specific activity than the first-generation supportless Pt black catalyst. Moreover, the porous Pt dendritic nanotubes were 6.1-fold and 4.8-fold more stable than the Pt/C and Pt black catalysts, respectively. Recently, Ding and co-workers prepared porous ternary Pt–Ni–P alloy nanotube arrays through a template-assisted electrodeposition method.[284] As shown in Fig. 23, the porous nanotube arrays showed a high electrochemical activity and long-term stability for methanol electrooxidation. These superior catalytic performances were ascribed to their porous and nanotubular structures, and the synergistic electronic effects of various elements. Huang *et al.*[285] prepared porous Pt_3Ni nanocrystals by simultaneously reducing platinum and nickel acetylacetonate organic salts by using *N*,*N*-dimethylformamide (DMF) as both solvent and reducing agent. PVP and phenol was used as surfactant and structure-directing agent, respectively. The porous Pt_3Ni nanocrystals were proved to have much better performance (in both durability and efficiency) toward the oxygen reduction reaction (ORR) than those of the commercial Pt analogs (commercial Pt

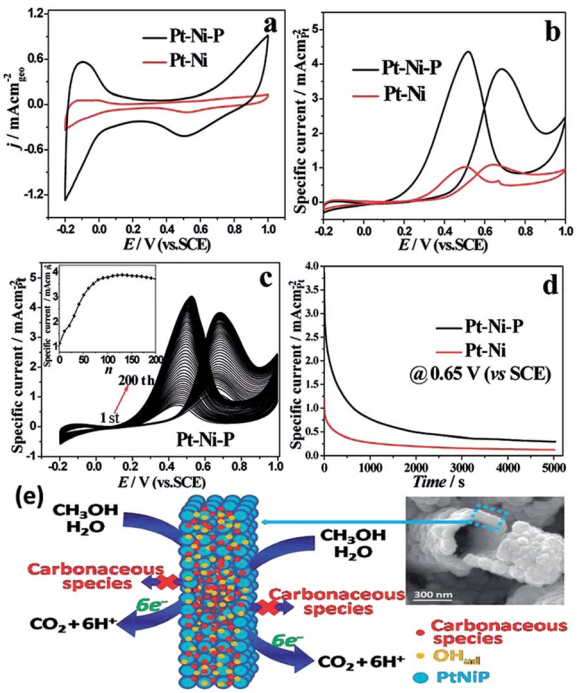

Fig. 23 (a) CVs of Pt–Ni–P and Pt–Ni NTAs in 0.5 M H_2SO_4 at 50 mV s^{-1}. (b) CVs of Pt–Ni–P and Pt–Ni NTAs in 0.5 M CH_3OH + 0.5 M H_2SO_4 at 50 mV s^{-1}. (c) CVs of Pt–Ni–P NTAs catalyst from the 1st to the 200th cycle (inset: change of peak current density with increasing cycle number). (d) Chronoamperometry curves of Pt–Ni–P and Pt–Ni NTAs in 0.5 M H_2SO_4 + 0.5 M CH_3OH at 50 mV s^{-1}. (e) Scheme for the almost complete oxidation of carbonaceous species generated during methanol electrooxidation in the porous walls of Pt–Ni–P NTAs. (Adapted with permission from ref. 284, copyright 2012, American Chemical Society.)

black and commercial Pt/C catalysts). Their superior performance in ORR was attributed to their high surface area, rough surface, and porous features.

4 Summary and outlook

In this review, synthesis mechanisms and the corresponding methods are demonstrated for the fabrication of porous noble metal units, including template methods, etching, galvanic replacement and so on. With these strategies, a broad range of noble metal NPs with porous structure can be designed selectively and synthesized. These tailored porous NPs with rough surface, high surface area, superior connectivity and mass diffusion properties have exhibited unique potentials in medical, SERS and catalytic applications.

Among the approaches developed for the synthesis of porous noble metals units, the Kirkendall effect can create pores in a diffusion couple, which is the generally accepted mechanism to explain the formation of hollows in the template-participated/sacrificed reaction, *e.g.* the galvanic reaction. However, a deep theoretical explanation focusing on the nanoscaled materials still needs to be developed further. In the case of so-called hard and soft template synthesis approaches, *e.g.* AAO, mesoporous zeolite, LLC and micelles, although the inner porosity can be well controlled, it is still hard to control the total size of the units to the nanoscale. The colloidal synthesis can provide a more direct and effective approach, which is more like a one-pot route compared to the tedious step-by-step template routes. However, how to control the pores distribution to enhance their mass conductivity as well as their phase structure, composition and total morphologies are still questions which have not been well resolved yet.

The porous structure of noble metals opens a broad field of potential applications. Porous Au NPs are ideal candidate as drug delivery carriers. Moreover, Ag and Au porous materials can show high SERS activities due to their structural features. The porous structures of Pt and Pd endow them with enhanced catalytic properties toward oxygen reduction. Furthermore, continued investigation into this area will likely yield many new porous noble metal units materials, which may improve a lot in this area.

Acknowledgements

The authors are grateful to Ms Lina Ma (The School of Foreign Studies, Xi'an Jiaotong University) for her help in revising the language of this manuscript. This work is supported by National Natural Science Foundation of China (no. 51271135), the program for New Century Excellent Talents in university (no. NCET-12-0455), the Fundamental Research Funds for the Central Universities and National Key Technology Research and Development Program of the Ministry of Science and Technology of China (no. 2012BAE06B08), and the project of Innovative Team of Shaanxi Province (no. 2013KCT-05).

Notes and references

1 R. J. White, R. Luque, V. L. Budarin, J. H. Clark and D. J. Macquarrie, *Chem. Soc. Rev.*, 2009, **38**, 481.
2 Y. Yamauchi, *J. Ceram. Soc. Jpn.*, 2013, **121**, 831.
3 C. Perego and R. Millini, *Chem. Soc. Rev.*, 2013, **42**, 3956.
4 C. M. A. Parlett, K. Wilson and A. F. Lee, *Chem. Soc. Rev.*, 2013, **42**, 3876.
5 R. Krishna, *Chem. Soc. Rev.*, 2012, **41**, 3099.
6 M. E. Davis, *Nature*, 2002, **417**, 813.
7 X. Zhang, X. Ke and H. Zhu, *Chem. – Eur. J.*, 2012, **18**, 8048.
8 A. B. Laursen, K. T. Hojholt, L. F. Lundegaard, S. B. Simonsen, S. Helveg, F. Schueth, M. Paul, J.-D. Grunwaldt, S. Kegnoes, C. H. Christensen and K. Egeblad, *Angew. Chem., Int. Ed.*, 2010, **49**, 3504.
9 J. Horacek, G. St'avova, V. Kelbichova and D. Kubicka, *Catal. Today*, 2013, **204**, 38.
10 J. C. Fierro-Gonzalez and B. C. Gates, *Langmuir*, 2005, **21**, 5693.
11 F. Durap, M. Rakap, M. Aydemir and S. Ozkar, *Appl. Catal., A*, 2010, **382**, 339.
12 V. Valtchev and L. Tosheva, *Chem. Rev.*, 2013, **113**, 6734.
13 G. D. Moon, S. W. Choi, X. Cai, W. Li, E. C. Cho, U. Jeong, L. V. Wang and Y. Xia, *J. Am. Chem. Soc.*, 2011, **133**, 4762.
14 J. Chen, M. Yang, Q. Zhang, E. C. Cho, C. M. Cobley, C. Kim, C. Glaus, L. V. Wang, M. J. Welch and Y. Xia, *Adv. Funct. Mater.*, 2010, **20**, 3684.
15 S. W. Choi, Y. Zhang and Y. Xia, *Angew. Chem., Int. Ed.*, 2010, **49**, 7904.
16 W. Li, X. Cai, C. Kim, G. Sun, Y. Zhang, R. Deng, M. Yang, J. Chen, S. Achilefu and L. V. Wang, *Nanoscale*, 2011, **3**, 1724.
17 S. Shukla, A. Priscilla, M. Banerjee, R. R. Bhonde, J. Ghatak, P. V. Satyam and M. Sastry, *Chem. Mater.*, 2005, **17**, 5000.
18 X. W. Teng, X. Y. Liang, S. Maksimuk and H. Yang, *Small*, 2006, **2**, 249.
19 F. Wang, C. Li, L.-D. Sun, C.-H. Xu, J. Wang, J. C. Yu and C.-H. Yan, *Angew. Chem., Int. Ed.*, 2012, **51**, 4872.
20 P. Sajanlal and T. Pradeep, *Langmuir*, 2010, **26**, 8901.
21 M. J. Mulvihill, X. Y. Ling, J. Henzie and P. Yang, *J. Am. Chem. Soc.*, 2010, **132**, 268.
22 L. Lu, A. Eychmüller, A. Kobayashi, Y. Hirano, K. Yoshida, Y. Kikkawa, K. Tawa and Y. Ozaki, *Langmuir*, 2006, **22**, 2605.
23 S.-a. Dong, S.-c. Yang and C. Tang, *Chem. Res. Chin. Univ.*, 2007, **23**, 500.
24 A. Chen and P. Holt-Hindle, *Chem. Rev.*, 2010, **110**, 3767.
25 Y. Xia, Y. Xiong, B. Lim and S. E. Skrabalak, *Angew. Chem., Int. Ed.*, 2009, **48**, 60.
26 Y. Xia, X. Xia, Y. Wang and S. Xie, *MRS Bull.*, 2013, **38**, 335.
27 G. R. Bourret, P. J. G. Goulet and R. B. Lennox, *Chem. Mater.*, 2011, **23**, 4954.
28 X. Gu, L. Xu, F. Tian and Y. Ding, *Nano Res.*, 2010, **2**, 386.
29 H. You, S. Yang, B. Ding and H. Yang, *Chem. Soc. Rev.*, 2013, **42**, 2880.
30 W. Yu, M. D. Porosoff and J. G. Chen, *Chem. Rev.*, 2012, **112**, 5780.
31 Z. Peng and H. Yang, *Nano Today*, 2009, **4**, 143.
32 M. R. Jones, K. D. Osberg, R. J. Macfarlane, M. R. Langille and C. A. Mirkin, *Chem. Rev.*, 2011, **111**, 3736.
33 Y. Liu, J. Goebl and Y. Yin, *Chem. Soc. Rev.*, 2013.

34 E. O. Kirkendall, *Trans. Am. Inst. Min. Metall. Eng.*, 1942, **147**, 104.
35 A. Smigelskas and E. Kirkendall, *Trans. Aime*, 1947, **171**, 130.
36 W. Wang, M. Dahl and Y. Yin, *Chem. Mater.*, 2013, **25**, 1179.
37 Y. D. Yin, R. M. Rioux, C. K. Erdonmez, S. Hughes, G. A. Somorjai and A. P. Alivisatos, *Science*, 2004, **304**, 711.
38 M. H. Kim, X. Lu, B. Wiley, E. P. Lee and Y. Xia, *J. Phys. Chem. C*, 2008, **112**, 7872.
39 Y. Sun, B. Wiley, Z.-Y. Li and Y. Xia, *J. Am. Chem. Soc.*, 2004, **126**, 9399.
40 Y. Sun and Y. Xia, *Adv. Mater.*, 2004, **16**, 264.
41 C. M. Cobley, D. J. Campbell and Y. Xia, *Adv. Mater.*, 2008, **20**, 748.
42 L. Au, Y. Chen, F. Zhou, P. H. Camargo, B. Lim, Z.-Y. Li, D. S. Ginger and Y. Xia, *Nano Res.*, 2008, **1**, 441.
43 J. Chen, J. M. McLellan, A. Siekkinen, Y. Xiong, Z.-Y. Li and Y. Xia, *J. Am. Chem. Soc.*, 2006, **128**, 14776.
44 G. Zhang, S. Sun, M. Cai, Y. Zhang, R. Li and X. Sun, *Sci. Rep.*, 2013, **3**, 526.
45 Y. Xia, W. Li, C. M. Cobley, J. Chen, X. Xia, Q. Zhang, M. Yang, E. C. Cho and P. K. Brown, *Acc. Chem. Res.*, 2011, **44**, 914.
46 Y. G. Sun and Y. N. Xia, *J. Am. Chem. Soc.*, 2004, **126**, 3892.
47 Y. Kim, H. J. Kim, Y. S. Kim, S. M. Choi, M. H. Seo and W. B. Kim, *J. Phys. Chem. C*, 2012, **116**, 18093.
48 D. Lee, H. Y. Jang, S. Hong and S. Park, *J. Colloid Interface Sci.*, 2012, **388**, 74.
49 S. M. Alia, G. Zhang, D. Kisailus, D. Li, S. Gu, K. Jensen and Y. Yan, *Adv. Funct. Mater.*, 2010, **20**, 3742.
50 J. Chen, B. Wiley, J. McLellan, Y. Xiong, Z.-Y. Li and Y. Xia, *Nano Lett.*, 2005, **5**, 2058.
51 E. Gonzalez, J. Arbiol and V. F. Puntes, *Science*, 2011, **334**, 1377.
52 W. Zhang, J. Yang and X. Lu, *ACS Nano*, 2012, 7397.
53 X. Hong, D. Wang, S. Cai, H. Rong and Y. Li, *J. Am. Chem. Soc.*, 2012, 18165.
54 E. Detsi, S. Punzhin, P. R. Onck and J. T. M. De Hosson, *J. Mater. Chem.*, 2012, **22**, 4588.
55 L. Kuai, B. Geng, S. Wang and Y. Sang, *Chem. – Eur. J.*, 2012, **18**, 9423.
56 H. M. Song, D. H. Anjum, R. Sougrat, M. N. Hedhili and N. M. Khashab, *J. Mater. Chem.*, 2012, **22**, 25003.
57 L. N. Zhuang, W. J. Wang, F. Hong, S. C. Yang, H. J. You, J. X. Fang and B. J. Ding, *J. Solid State Chem.*, 2012, **191**, 239.
58 D. R. Lide, *CRC Handbook of Chemistry and Physics*, 84th edn, CRC Press, Boca Raton, FL, 2004.
59 J. W. Hong, S. W. Kang, B.-S. Choi, D. Kim, S. B. Lee and S. W. Han, *ACS Nano*, 2012, **6**, 2410.
60 H. Zhang, M. Jin, H. Liu, J. Wang, M. J. Kim, D. Yang, Z. Xie, J. Liu and Y. Xia, *ACS Nano*, 2011, **5**, 8212.
61 H. Zhang, M. Jin, J. Wang, W. Li, P. H. C. Camargo, M. J. Kim, D. Yang, Z. Xie and Y. Xia, *J. Am. Chem. Soc.*, 2011, **133**, 6078.
62 S. Xie, H.-C. Peng, N. Lu, J. Wang, M. J. Kim, Z. Xie and Y. Xia, *J. Am. Chem. Soc.*, 2013, **135**, 16658.
63 R. Pasricha, T. Bala, A. V. Biradar, S. Umbarkar and M. Sastry, *Small*, 2009, **5**, 1467.
64 H. P. Liang, H. M. Zhang, J. S. Hu, Y. G. Guo, L. J. Wan and C. L. Bai, *Angew. Chem., Int. Ed.*, 2004, **43**, 1540.
65 Y. Vasquez, A. K. Sra and R. E. Schaak, *J. Am. Chem. Soc.*, 2005, **127**, 12504.
66 M. Mohl, D. Dobo, A. Kukovecz, Z. Konya, K. Kordas, J. Wei, R. Vajtai and P. M. Ajayan, *J. Phys. Chem. C*, 2011, **115**, 9403.
67 A. P. O'Mullane, S. J. Ippolito, A. M. Bond and S. K. Bhargava, *Electrochem. Commun.*, 2010, **12**, 611.
68 M. Clay, Q. Cui, Y. Sha, J. Chen, A. J. Rondinone, Z. Wu, J. Chen and Z. Gul, *Mater. Lett.*, 2012.
69 B. Mayers, X. C. Jiang, D. Sunderland, B. Cattle and Y. N. Xia, *J. Am. Chem. Soc.*, 2003, **125**, 13364.
70 Z. H. Lin, M. H. Lin and H. T. Chang, *Chem. – Eur. J.*, 2009, **15**, 4656.
71 Z. H. Lin and H. T. Chang, *Langmuir*, 2008, **24**, 365.
72 H. W. Liang, S. Liu, J. Y. Gong, S. B. Wang, L. Wang and S. H. Yu, *Adv. Mater.*, 2009, **21**, 1850.
73 H.-W. Liang, X. Cao, F. Zhou, C.-H. Cui, W.-J. Zhang and S.-H. Yu, *Adv. Mater.*, 2011, **23**, 1467.
74 Y. Ji, S. Yang, S. Guo, X. Song, B. Ding and Z. Yang, *Colloids Surf., A*, 2010, **372**, 204.
75 K. Cai, Z. Lv, K. Chen, L. Huang, J. Wang, F. Shao, Y. Wang and H. Han, *Chem. Commun.*, 2013, **49**, 6024.
76 A. Ben Moshe and G. Markovich, *Chem. Mater.*, 2011, **23**, 1239.
77 J. H. Yang, L. M. Qi, C. H. Lu, J. M. Ma and H. M. Cheng, *Angew. Chem., Int. Ed.*, 2005, **44**, 598.
78 T. D. Lazzara, G. R. Bourret, R. B. Lennox and T. G. M. van de Ven, *Chem. Mater.*, 2009, **21**, 2020.
79 G. R. Bourret and R. B. Lennox, *ACS Appl. Mater. Interfaces*, 2010, **2**, 3745.
80 Y. Bi, S. Ouyang, J. Cao and J. Ye, *Phys. Chem. Chem. Phys.*, 2011, **13**, 10071.
81 Y. Bi, S. Ouyang, N. Umezawa, J. Cao and J. Ye, *J. Am. Chem. Soc.*, 2011, **133**, 6490.
82 C. T. Dinh, T. D. Nguyen, F. Kleitz and T. O. Do, *Chem. Commun.*, 2011, **47**, 7797.
83 X. Luo, S. Lian, L. Wang, S. Yang, Z. Yang, B. Ding and X. Song, *CrystEngComm*, 2013, **15**, 2588.
84 F. Hong, S. Sun, H. You, S. Yang, J. Fang, S. Guo, Z. Yang, B. Ding and X. Song, *Cryst. Growth Des.*, 2011, **11**, 3694.
85 J. Fang, S. Lebedkin, S. Yang and H. Hahn, *Chem. Commun.*, 2011, **47**, 5157.
86 C. H. Kuo and M. H. Huang, *Nano Today*, 2010, **5**, 106.
87 X.-W. Liu, F.-Y. Wang, F. Zhen and J.-R. Huang, *RSC Adv.*, 2012, **2**, 7647.
88 V. Vongsavat, B. M. Vittur, W. W. Bryan, J.-H. Kim and T. R. Lee, *ACS Appl. Mater. Interfaces*, 2011, **3**, 3616.
89 Q. Li, P. Xu, B. Zhang, G. Wu, H. Zhao, E. Fu and H.-L. Wang, *Nanoscale*, 2013, **5**, 7397.
90 K. W. Kim, S. M. Kim, S. Choi, J. Kim and I. S. Lee, *ACS Nano*, 2012, **6**, 5122.
91 Y. Yamauchi and K. Kuroda, *Chem. – Asian J.*, 2008, **3**, 664.
92 H. Wang, H. Y. Jeong, M. Imura, L. Wang, L. Radhakrishnan, N. Fujita, T. Castle, O. Terasaki and Y. Yamauchi, *J. Am. Chem. Soc.*, 2011, **133**, 14526.

93 H. Wang, M. Imura, Y. Nemoto, S.-E. Park and Y. Yamauchi, *Chem. – Asian J.*, 2012, **7**, 802.
94 P. Karthika, H. Ataee-Esfahani, H. Wang, M. A. Francis, H. Abe, N. Rajalakshmi, K. S. Dhathathreyan, D. Arivuoli and Y. Yamauchi, *Chem. – Asian J.*, 2013, **8**, 902.
95 P. Karthika, H. Ataee-Esfahani, Y.-H. Deng, K. C. W. Wu, N. Rajalakshmi, K. S. Dhathathreyan, D. Arivuoli, K. Ariga and Y. Yamauchi, *Chem. Lett.*, 2013, **42**, 447.
96 J. Kibsgaard, Y. Gorlin, Z. Chen and T. F. Jaramillo, *J. Am. Chem. Soc.*, 2012, **134**, 7758.
97 M. Rauber, I. Alber, S. Mueller, R. Neumann, O. Picht, C. Roth, A. Schoekel, M. E. Toimil-Molares and W. Ensinger, *Nano Lett.*, 2011, **11**, 2304.
98 A. Takai, Y. Yamauchi and K. Kuroda, *Chem. Commun.*, 2008, 4171.
99 Y. Yamauchi, A. Takai, M. Komatsu, M. Sawada, T. Ohsuna and K. Kuroda, *Chem. Mater.*, 2008, **20**, 1004.
100 J. Xu, G. Chen, R. Yan, D. Wang, M. Zhang, W. Zhang and P. Sun, *Macromolecules*, 2011, **44**, 3730.
101 G. S. Attard, P. N. Bartlett, N. R. B. Coleman, J. M. Elliott, J. R. Owen and J. H. Wang, *Science*, 1997, **278**, 838.
102 Y. Yamauchi, T. Momma, M. Fuziwara, S. S. Nair, T. Ohsuna, O. Terasaki, T. Osaka and K. Kuroda, *Chem. Mater.*, 2005, **17**, 6342.
103 Y. Yamauchi, A. Sugiyama, R. Morimoto, A. Takai and K. Kuroda, *Angew. Chem., Int. Ed.*, 2008, **47**, 5371.
104 Y. Yamauchi, A. Takai, T. Nagaura, S. Inoue and K. Kuroda, *J. Am. Chem. Soc.*, 2008, **130**, 5426.
105 L. Li, Z. Wang, T. Huang, J. Xie and L. Qi, *Langmuir*, 2010, **26**, 12330.
106 M. Pan, H. Sun, J. W. Lim, S. R. Bakaul, Y. Zeng, S. Xing, T. Wu, Q. Yan and H. Chen, *Chem. Commun.*, 2012, **48**, 1440.
107 M. Pan, S. Xing, T. Sun, W. Zhou, M. Sindoro, H. H. Teo, Q. Yan and H. Chen, *Chem. Commun.*, 2010, **46**, 7112.
108 C. Yuan, L. Zhong, C. Yang, G. Chen, B. Jiang, Y. Deng, Y. Xu, W. Luo, B. Zeng, J. Liu and L. Dai, *J. Mater. Chem.*, 2012, **22**, 7108.
109 D. B. Robinson, S. J. Fares, M. D. Ong, I. Arslan, M. E. Langham, K. L. Tran and W. M. Clift, *Int. J. Hydrogen Energy*, 2009, **34**, 5585.
110 Y. Song, Y. Yang, C. J. Medforth, E. Pereira, A. K. Singh, H. Xu, Y. Jiang, C. J. Brinker, F. van Swol and J. A. Shelnutt, *J. Am. Chem. Soc.*, 2004, **126**, 635.
111 Y. Song, W. A. Steen, D. Peña, Y.-B. Jiang, C. J. Medforth, Q. Huo, J. L. Pincus, Y. Qiu, D. Y. Sasaki and J. E. Miller, *Chem. Mater.*, 2006, **18**, 2335.
112 Y. Song, R. M. Garcia, R. M. Dorin, H. Wang, Y. Qiu and J. A. Shelnutt, *Angew. Chem., Int. Ed.*, 2006, **45**, 8126.
113 Y. Song, R. M. Dorin, R. M. Garcia, Y.-B. Jiang, H. Wang, P. Li, Y. Qiu, F. van Swol, J. E. Miller and J. A. Shelnutt, *J. Am. Chem. Soc.*, 2008, **130**, 12602.
114 Y. J. Song, Y. B. Jiang, H. R. Wang, D. A. Pena, Y. Qiu, J. E. Miller and J. A. Shelnutt, *Nanotechnology*, 2006, **17**, 1300.
115 Y. Song, M. A. Hickner, S. R. Challa, R. M. Dorin, R. M. Garcia, H. Wang, Y.-B. Jiang, P. Li, Y. Qiu, F. van Swol, C. J. Medforth, J. E. Miller, T. Nwoga, K. Kawahara, W. Li and J. A. Shelnutt, *Nano Lett.*, 2009, **9**, 1534.
116 R. M. Garcia, Y. Song, R. M. Dorin, H. Wang, P. Li, Y. Qiu, F. van Swol and J. A. Shelnutt, *Chem. Commun.*, 2008, 2535.
117 R. M. Garcia, Y. Song, R. M. Dorin, H. Wang, A. M. Moreno, Y.-B. Jiang, Y. Tian, Y. Qiu, C. J. Medforth, E. N. Coker, F. van Swol, J. E. Miller and J. A. Shelnutt, *Phys. Chem. Chem. Phys.*, 2011, **13**, 4846.
118 H. Wang, Y. Song, C. J. Medforth and J. A. Shelnutt, *J. Am. Chem. Soc.*, 2006, **128**, 9284.
119 K. S. Choi, E. W. McFarland and G. D. Stucky, *Adv. Mater.*, 2003, **15**, 2018.
120 H. Wang, L. Wang, T. Sato, Y. Sakamoto, S. Tominaka, K. Miyasaka, N. Miyamoto, Y. Nemoto, O. Terasaki and Y. Yamauchi, *Chem. Mater.*, 2012, **24**, 1591.
121 H. Wang, M. Imura, Y. Nemoto, L. Wang, H. Y. Jeong, T. Yokoshima, O. Terasaki and Y. Yamauchi, *Chem. – Eur. J.*, 2012, **18**, 13142.
122 C. Li and Y. Yamauchi, *Chem. – Eur. J.*, 2014, **20**, 729.
123 C. Li, T. Sato and Y. Yamauchi, *Angew. Chem., Int. Ed.*, 2013, **52**, 8050.
124 H. Ataee-Esfahani, J. Liu, M. Hu, N. Miyamoto, S. Tominaka, K. C. W. Wu and Y. Yamauchi, *Small*, 2013, **9**, 1047.
125 Y. Lu and W. Chen, *Chem. Commun.*, 2011, **47**, 2541.
126 R. Xia, J. L. Wang, R. Wang, X. Li, X. Zhang, X.-Q. Feng and Y. Ding, *Nanotechnology*, 2010, 21.
127 H. M. Chen, R.-S. Liu, M.-Y. Lo, S.-C. Chang, L.-D. Tsai, Y.-M. Peng and J.-F. Lee, *J. Phys. Chem. C*, 2008, **112**, 7522.
128 X. Lu, L. Au, J. McLellan, Z.-Y. Li, M. Marquez and Y. Xia, *Nano Lett.*, 2007, **7**, 1764.
129 X. Huang, S. Tang, J. Yang, Y. Tan and N. Zheng, *J. Am. Chem. Soc.*, 2011, **133**, 15946.
130 S.-H. Yoo, L. Liu, S. H. Cho and S. Park, *Chem. – Asian J.*, 2012, **7**, 2937.
131 Y. J. Xiong, B. Wiley, J. Y. Chen, Z. Y. Li, Y. D. Yin and Y. N. Xia, *Angew. Chem., Int. Ed.*, 2005, **44**, 7913.
132 N. Fan, Y. Yang, W. Wang, L. Zhang, W. Chen, C. Zou and S. Huang, *ACS Nano*, 2012, **6**, 4072.
133 H. Wu, P. Wang, H. He and Y. Jin, *Nano Res.*, 2012, **5**, 135.
134 M. Shao, B. H. Smith, S. Guerrero, L. Protsailo, D. Su, K. Kaneko, J. H. Odell, M. P. Humbert, K. Sasaki, J. Marzullo and R. M. Darling, *Phys. Chem. Chem. Phys.*, 2013, **15**, 15078.
135 Z. Peng, J. Wu and H. Yang, *Chem. Mater.*, 2010, **22**, 1098.
136 Z. Peng, H. You, J. Wu and H. Yang, *Nano Lett.*, 2010, **10**, 1492.
137 M. Shao, K. Shoemaker, A. Peles, K. Kaneko and L. Protsailo, *J. Am. Chem. Soc.*, 2010, **132**, 9253.
138 M. Oezaslan, M. Heggen and P. Strasser, *J. Am. Chem. Soc.*, 2012, **134**, 514.
139 Y. J. Xiong, J. M. McLellan, J. Y. Chen, Y. D. Yin, Z. Y. Li and Y. N. Xia, *J. Am. Chem. Soc.*, 2005, **127**, 17118.
140 B. Wiley, T. Herricks, Y. G. Sun and Y. N. Xia, *Nano Lett.*, 2004, **4**, 1733.
141 S. Peng and Y. Sun, *Chem. Mater.*, 2010, **22**, 6272.

142 M. R. Langille, M. L. Personick, J. Zhang and C. A. Mirkin, *J. Am. Chem. Soc.*, 2011, **133**, 10414.
143 C. J. DeSantis, A. C. Sue, M. M. Bower and S. E. Skrabalak, *ACS Nano*, 2012, **6**, 2617.
144 Y. Ma, Q. Kuang, Z. Jiang, Z. Xie, R. Huang and L. Zheng, *Angew. Chem., Int. Ed.*, 2008, **47**, 8901.
145 J. Zhang, L. Zhang, S. Xie, Q. Kuang, X. Han, Z. Xie and L. Zheng, *Chem. – Eur. J.*, 2011, **17**, 9915.
146 M. McEachran, D. Keogh, B. Pietrobon, N. Cathcart, I. Gourevich, N. Coombs and V. Kitaev, *J. Am. Chem. Soc.*, 2011, **133**, 8066.
147 T. Graham, *Philos. Trans. R. Soc. London*, 1861, **151**, 183.
148 *Nanomaterials for Life Sciences*, ed. C. S. S. R. Kumar, WILEY-VCH Verlag GmbH & Co., Weinheim, 2008.
149 S. Maksimuk, X. Teng and H. Yang, *J. Phys. Chem. C*, 2007, **111**, 14312.
150 M. Rycenga, C. M. Cobley, J. Zeng, W. Li, C. H. Moran, Q. Zhang, D. Qin and Y. Xia, *Chem. Rev.*, 2011, **111**, 3669.
151 S. Guo and E. Wang, *Nano Today*, 2011, **6**, 240.
152 T. K. Sau, A. L. Rogach, F. Jaeckel, T. A. Klar and J. Feldmann, *Adv. Mater.*, 2010, **22**, 1805.
153 J. Gu, Y.-W. Zhang and F. Tao, *Chem. Soc. Rev.*, 2012, **41**, 8050.
154 Q. Yuan and X. Wang, *Nanoscale*, 2010, **2**, 2328.
155 W. Niu and G. Xu, *Nano Today*, 2011, **6**, 265.
156 B. Viswanath, P. Kundu, A. HaIder and N. Ravishankar, *J. Phys. Chem. C*, 2009, **113**, 16866.
157 A. R. Tao, S. Habas and P. Yang, *Small*, 2008, **4**, 310.
158 B. Y. Xia, N. Wan Theng, H. B. Wu, X. Wang and X. W. Lou, *Angew. Chem., Int. Ed.*, 2012, **51**, 7213.
159 M. A. Watzky and R. G. Finke, *J. Am. Chem. Soc.*, 1997, **119**, 10382.
160 Q. Yuan, Z. Zhou, J. Zhuang and X. Wang, *Inorg. Chem.*, 2010, **49**, 5515.
161 N. Zettsu, J. M. McLellan, B. Wiley, Y. D. Yin, Z. Y. Li and Y. N. Xia, *Angew. Chem., Int. Ed.*, 2006, **45**, 1288.
162 L. Wang, H. Wang, Y. Nemoto and Y. Yamauchi, *Chem. Mater.*, 2010, **22**, 2835.
163 L. Wang and Y. Yamauchi, *Chem. Mater.*, 2009, **21**, 3562.
164 L. Wang, S. Guo, J. Zhai and S. Dong, *J. Phys. Chem. C*, 2008, **112**, 13372.
165 Y. W. Lee, M. Kim and S. W. Han, *Chem. Commun.*, 2010, **46**, 1535.
166 H.-T. Zhang, J. Ding and G.-M. Chow, *Langmuir*, 2008, **24**, 375.
167 B. Lim, M. J. Jiang, P. H. C. Camargo, E. C. Cho, J. Tao, X. M. Lu, Y. M. Zhu and Y. N. Xia, *Science*, 2009, **324**, 1302.
168 Z. M. Peng and H. Yang, *J. Am. Chem. Soc.*, 2009, **131**, 7542.
169 L. Wang and Y. Yamauchi, *J. Am. Chem. Soc.*, 2010, **132**, 13636.
170 L. Wang, Y. Nemoto and Y. Yamauchi, *J. Am. Chem. Soc.*, 2011, **133**, 9674.
171 K. M. Yeo, S. Choi, R. M. Anisur, J. Kim and I. S. Lee, *Angew. Chem., Int. Ed.*, 2011, **50**, 745.
172 S. Guo, J. Li, S. Dong and E. Wang, *J. Phys. Chem. C*, 2010, **114**, 15337.
173 S. Guo, S. Dong and E. Wang, *ACS Nano*, 2010, **4**, 547.
174 B. Lim and Y. Xia, *Angew. Chem., Int. Ed.*, 2011, **50**, 76.
175 J. H. Shim, J. Kim, C. Lee and Y. Lee, *Chem. Mater.*, 2011, **23**, 4694.
176 L. Wang and Y. Yamauchi, *Chem. Mater.*, 2011, **23**, 2457.
177 H. Ataee-Esfahani, L. Wang, Y. Nemoto and Y. Yamauchi, *Chem. Mater.*, 2010, **22**, 6310.
178 H. Yang, *Angew. Chem., Int. Ed.*, 2011, **50**, 2674.
179 H. Ataee-Esfahani, L. Wang and Y. Yamauchi, *Chem. Commun.*, 2010, **46**, 3684.
180 L. Zhang, J. Zhang, Z. Jiang, S. Xie, M. Jin, X. Han, Q. Kuang, Z. Xie and L. Zheng, *J. Mater. Chem.*, 2011, **21**, 9620.
181 D. Wang, P. Zhao and Y. Li, *Sci. Rep.*, 2011, **1**, 37.
182 L. Liu and E. Pippel, *Angew. Chem., Int. Ed.*, 2011, **50**, 2729.
183 E. A. Anumol, A. Halder, C. Nethravathi, B. Viswanath and N. Ravishankar, *J. Mater. Chem.*, 2011, **21**, 8721.
184 Z. Zhang, K. L. More, K. Sun, Z. Wu and W. Li, *Chem. Mater.*, 2011, **23**, 1570.
185 G. Xiang, J. He, T. Li, J. Zhuang and X. Wang, *Nanoscale*, 2011, **3**, 3737.
186 H. Kobayashi, B. Lim, J. Wang, P. H. C. Camargo, T. Yu, M. J. Kim and Y. Xia, *Chem. Phys. Lett.*, 2010, **494**, 249.
187 Y. W. Lee, M. Kim, Y. Kim, S. W. Kang, J.-H. Lee and S. W. Han, *J. Phys. Chem. C*, 2010, **114**, 7689.
188 L. Zhang, W. Niu and G. Xu, *Nanoscale*, 2011, **3**, 678.
189 L. Wang and Y. Yamauchi, *Chem. – Asian J.*, 2010, **5**, 2493.
190 Y. Zhang, M. Janyasupab, C.-W. Liu, X. Li, J. Xu and C.-C. Liu, *Adv. Funct. Mater.*, 2012, **22**, 3570.
191 H. Ataee-Esfahani, M. Imura and Y. Yamauchi, *Angew. Chem., Int. Ed.*, 2013, **52**, 13611.
192 R. L. Penn and J. F. Banfield, *Science*, 1998, **281**, 969.
193 A. W. Xu, M. Antonietti, H. Colfen and Y. P. Fang, *Adv. Funct. Mater.*, 2006, **16**, 903.
194 V. M. Yuwono, N. D. Burrows, J. A. Soltis and R. L. Penn, *J. Am. Chem. Soc.*, 2010, **132**, 2163.
195 J. Wang, X.-B. Zhang, Z.-L. Wang, L.-M. Wang, W. Xing and X. Liu, *Nanoscale*, 2012, **4**, 1549.
196 S. Tang, S. Vongehr, Z. Zheng, H. Ren and X. Meng, *Nanotechnology*, 2012, **23**, 255606.
197 L. Zhang, Q. Sui, T. Tang, Y. Chen, Y. Zhou, Y. Tang and T. Lu, *Electrochem. Commun.*, 2013, **32**, 43.
198 B. Viswanath, S. Patra, N. Munichandraiah and N. Ravishankar, *Langmuir*, 2009, **25**, 3115.
199 Y. Huang, M. Yin, X. Zhou, C. Liu and W. Xing, *Nanotechnology*, 2012, **23**, 35605.
200 Q. Shen, L. Jiang, H. Zhang, Q. Min, W. Hou and J.-J. Zhu, *J. Phys. Chem. C*, 2008, **112**, 16385.
201 L. Wang, M. Imura and Y. Yamauchi, *ACS Appl. Mater. Interfaces*, 2012, **4**, 2865.
202 S. Y. Gao, H. J. Zhang, X. D. Liu, X. M. Wang, D. H. Sun, C. Y. Peng and G. L. Zheng, *Nanotechnology*, 2006, **17**, 1599.
203 C.-L. Lee, Y.-J. Chao, C.-H. Chen, H.-P. Chiou and C.-C. Syu, *Int. J. Hydrogen Energy*, 2011, **36**, 15045.
204 G. Fu, W. Han, L. Yao, J. Lin, S. Wei, Y. Chen, Y. Tang, Y. Zhou, T. Lu and X. Xia, *J. Mater. Chem.*, 2012, **22**, 17604.
205 G. Fu, K. Wu, J. Lin, Y. Tang, Y. Chen, Y. Zhou and T. Lu, *J. Phys. Chem. C*, 2013, **117**, 9826.

206 X. Teng, S. Maksimuk, S. Frommer and H. Yang, *Chem. Mater.*, 2007, **19**, 36.
207 H. You, Y. Ji, L. Wang, S. Yang, Z. Yang, J. Fang, X. Song and B. Ding, *J. Mater. Chem.*, 2012, **22**, 1998.
208 M. Nogami, R. Koike, R. Jalem, G. Kawamura, Y. Yang and Y. Sasaki, *J. Phys. Chem. Lett.*, 2010, **1**, 568.
209 B. Lim, X. Lu, M. Jiang, P. H. C. Camargo, E. C. Cho, E. P. Lee and Y. Xia, *Nano Lett.*, 2008, **8**, 4043.
210 S.-C. Yang, X.-W. Wan, Y.-T. Ji, L.-Q. Wang, X.-P. Song, B.-J. Ding and Z.-M. Yang, *CrystEngComm*, 2010, **12**, 3291.
211 S. Yang, T. Zhang, L. Zhang, Q. Wang, R. Zhang and B. Ding, *Nanotechnology*, 2006, **17**, 5639.
212 S. Yang, Y. Wang, Q. Wang, R. Zhang, Z. Yang, Y. Guo and B. Ding, *Cryst. Growth Des.*, 2007, **7**, 2258.
213 W. Tong, S. Yang and B. Ding, *Colloids Surf., A*, 2009, **340**, 131.
214 Y. Tao, J. Han, C. Ye, T. Thomas and H. Dou, *J. Mater. Chem.*, 2012, **22**, 18864.
215 J. You, G. Zhang and C. Li, *ACS Nano*, 2010, **4**, 1033.
216 A. P. Esser-Kahn, S. A. Odom, N. R. Sottos, S. R. White and J. S. Moore, *Macromolecules*, 2011, **44**, 5539.
217 H. Park, J. Yang, J. Lee, S. Haam, I.-H. Choi and K.-H. Yoo, *ACS Nano*, 2009, **3**, 2919.
218 Y. Ma, X. Liang, S. Tong, G. Bao, Q. Ren and Z. Dai, *Adv. Funct. Mater.*, 2013, **23**, 815.
219 E. Boisselier and D. Astruc, *Chem. Soc. Rev.*, 2009, **38**, 1759.
220 C. M. Cobley, J. Chen, E. C. Cho, L. V. Wang and Y. Xia, *Chem. Soc. Rev.*, 2011, **40**, 44.
221 X. Lu, H.-Y. Tuan, J. Chen, Z.-Y. Li, B. A. Korgel and Y. Xia, *J. Am. Chem. Soc.*, 2007, **129**, 1733.
222 K. Niikura, N. Iyo, T. Higuchi, T. Nishio, H. Jinnai, N. Fujitani and K. Ijiro, *J. Am. Chem. Soc.*, 2012, **134**, 7632.
223 K. Niikura, N. Iyo, Y. Matsuo, H. Mitomo and K. Ijiro, *ACS Appl. Mater. Interfaces*, 2013, **5**, 3900.
224 S. R. Sershen, S. L. Westcott, N. J. Halas and J. L. West, *J. Biomed. Mater. Res.*, 2000, **51**, 293.
225 C. Loo, A. Lowery, N. J. Halas, J. West and R. Drezek, *Nano Lett.*, 2005, **5**, 709.
226 C. Zhou, T.-H. Tsai, D. C. Adler, H.-C. Lee, D. W. Cohen, A. Mondelblatt, Y. Wang, J. L. Connolly and J. G. Fujimoto, *Opt. Lett.*, 2010, **35**, 700.
227 M.-R. Choi, K. J. Stanton-Maxey, J. K. Stanley, C. S. Levin, R. Bardhan, D. Akin, S. Badve, J. Sturgis, J. P. Robinson, R. Bashir, N. J. Halas and S. E. Clare, *Nano Lett.*, 2007, **7**, 3759.
228 Y. W. Wang, X. Y. Xie, X. D. Wang, G. Ku, K. L. Gill, D. P. O'Neal, G. Stoica and L. V. Wang, *Nano Lett.*, 2004, **4**, 1689.
229 K. H. Song, C. Kim, C. M. Cobley, Y. Xia and L. V. Wang, *Nano Lett.*, 2009, **9**, 183.
230 S. Guo, Y. Fang, S. Dong and E. Wang, *J. Phys. Chem. C*, 2007, **111**, 17104.
231 X. Gong, Y. Bao, C. Qiu and C. Jiang, *Chem. Commun.*, 2012, **48**, 7003.
232 L. Zhang, X. Gong, Y. Bao, Y. Zhao, M. Xi, C. Jiang and H. Fong, *Langmuir*, 2012.
233 M. Rycenga, X. Xia, C. H. Moran, F. Zhou, D. Qin, Z. Y. Li and Y. Xia, *Angew. Chem., Int. Ed.*, 2011, **50**, 5473.
234 M. Fan, G. F. S. Andrade and A. G. Brolo, *Anal. Chim. Acta*, 2011, **693**, 7.
235 S. L. Kleinman, E. Ringe, N. Valley, K. L. Wustholz, E. Phillips, K. A. Scheidt, G. C. Schatz and R. P. Van Duyne, *J. Am. Chem. Soc.*, 2011, **133**, 4115.
236 S. J. Guo, S. J. Dong and E. K. Wang, *ACS Nano*, 2010, **4**, 547.
237 H. Chen, G. Wei, A. Ispas, S. G. Hickey and A. Eychmueller, *J. Phys. Chem. C*, 2010, **114**, 21976.
238 B. Guo, G. Han, M. Li and S. Zhao, *Thin Solid Films*, 2010, **518**, 3228.
239 R. A. Halvorson and P. J. Vikesland, *Environ. Sci. Technol.*, 2010, **44**, 7749.
240 J. Fang, S. Du, S. Lebedkin, Z. Li, R. Kruk, M. Kappes and H. Hahn, *Nano Lett.*, 2010, **10**, 5006.
241 G. H. Jeong, Y. W. Lee, M. Kim and S. W. Han, *J. Colloid Interface Sci.*, 2009, **329**, 97.
242 H. Liang, Z. Li, W. Wang, Y. Wu and H. Xu, *Adv. Mater.*, 2009, **21**, 4614.
243 J. P. Camden, J. A. Dieringer, Y. Wang, D. J. Masiello, L. D. Marks, G. C. Schatz and R. P. Van Duyne, *J. Am. Chem. Soc.*, 2008, **130**, 12616.
244 J. A. Dieringer, K. L. Wustholz, D. J. Masiello, J. P. Camden, S. L. Kleinman, G. C. Schatz and R. P. Van Duyne, *J. Am. Chem. Soc.*, 2009, **131**, 849.
245 N. Tian, Z.-Y. Zhou, S.-G. Sun, L. Cui, B. Ren and Z.-Q. Tian, *Chem. Commun.*, 2006, 4090.
246 M. Canamares, J. Garcia-Ramos, J. Gomez-Varga, C. Domingo and S. Sanchez-Cortes, *Langmuir*, 2005, **21**, 8546.
247 K. Kneipp, Y. Wang, H. Kneipp, L. T. Perelman, I. Itzkan, R. R. Dasari and M. S. Feld, *Phys. Rev. Lett.*, 1997, **78**, 1667.
248 S. Nie and S. R. Emory, *Science*, 1997, **275**, 1102.
249 D.-P. Yang, S. Chen, P. Huang, X. Wang, W. Jiang, O. Pandoli and D. Cui, *Green Chem.*, 2010, **12**, 2038.
250 *System Design for Transport Applications. Handbook of Fuel Cells*, ed. A. Lamm and J. Müller, John Wiley & Sons, Ltd., Weinheim, 2010.
251 J. Zhang and C. M. Li, *Chem. Soc. Rev.*, 2012, **41**, 7016.
252 Y. Qiao and C. M. Li, *J. Mater. Chem.*, 2011, **21**, 4027.
253 L. Zhang, J. Zhang, Q. Kuang, S. Xie, Z. Jiang, Z. Xie and L. Zheng, *J. Am. Chem. Soc.*, 2011, **133**, 17114.
254 J.-D. Qiu, G.-C. Wang, R.-P. Liang, X.-H. Xia and H.-W. Yu, *J. Phys. Chem. C*, 2011, **115**, 15639.
255 E. Antolini and J. Perez, *J. Mater. Sci.*, 2011, **46**, 4435.
256 E. Casado-Rivera, D. J. Volpe, L. Alden, C. Lind, C. Downie, T. Vazquez-Alvarez, A. C. D. Angelo, F. J. DiSalvo and H. D. Abruna, *J. Am. Chem. Soc.*, 2004, **126**, 4043.
257 F. Ye, H. Liu, W. Hu, J. Zhong, Y. Chen, H. Cao and J. Yang, *Dalton Trans.*, 2012, **41**, 2898.
258 W. He, X. Wu, J. Liu, K. Zhang, W. Chu, L. Feng, X. Hu, W. Zhou and S. Xie, *J. Phys. Chem. C*, 2009, **113**, 10505.
259 B. Lim, M. Jiang, P. H. C. Camargo, E. C. Cho, J. Tao, X. Lu, Y. Zhu and Y. Xia, *Science*, 2009, **324**, 1302.
260 J. Qu, H. Liu, F. Ye, W. Hu and J. Yang, *Int. J. Hydrogen Energy*, 2012, **37**, 13191.

261 M. Shao, K. Shoemaker, A. Peles, K. Kaneko and L. Protsailo, *J. Am. Chem. Soc.*, 2010, **132**, 9253.
262 J. N. Tiwari, F.-M. Pan, R. N. Tiwari and S. K. Nandi, *Chem. Commun.*, 2008, 6516.
263 C. Xu, L. Wang, X. Mu and Y. Ding, *Langmuir*, 2010, **26**, 7437.
264 C. Xu, R. Wang, M. Chen, Y. Zhang and Y. Ding, *Phys. Chem. Chem. Phys.*, 2010, **12**, 239.
265 J. Yang, J. Yang and J. Y. Ying, *ACS Nano*, 2012, **6**, 9373.
266 H. Zhang, X. Xu, P. Gu, C. Li, P. Wu and C. Cai, *Electrochim. Acta*, 2011, **56**, 7064.
267 D. Wang and Y. Li, *Adv. Mater.*, 2011, **23**, 1044.
268 S. Guo and E. Wang, *Acc. Chem. Res.*, 2011, **44**, 491.
269 Y. Bing, H. Liu, L. Zhang, D. Ghosh and J. Zhang, *Chem. Soc. Rev.*, 2010, **39**, 2184.
270 Q. Shen, Q. Min, J. Shi, L. Jiang, J.-R. Zhang, W. Hou and J.-J. Zhu, *J. Phys. Chem. C*, 2009, **113**, 1267.
271 C. Koenigsmann, A. C. Santulli, K. P. Gong, M. B. Vukmirovic, W. P. Zhou, E. Sutter, S. S. Wong and R. R. Adzic, *J. Am. Chem. Soc.*, 2011, **133**, 9783.
272 H. Zhao, J. Wu, H. You, S. Yang, B. Ding, Z. Yang, X. Song and H. Yang, *J. Mater. Chem.*, 2012, **22**, 12046.
273 H. Zhao, S. Yang, H. You, Y. Wu and B. Ding, *Green Chem.*, 2012, **14**, 3197.
274 S. Yang, Z. Peng and H. Yang, *Adv. Funct. Mater.*, 2008, **18**, 2745.
275 J. L. Fernández, V. Raghuveer, A. Manthiram and A. J. Bard, *J. Am. Chem. Soc.*, 2005, **127**, 13100.
276 M. Sanles-Sobrido, M. A. Correa-Duarte, S. Carregal-Romero, B. Rodriguez-Gonzalez, R. A. Alvarez-Puebla, P. Herves and L. M. Liz-Marzan, *Chem. Mater.*, 2009, **21**, 1531.
277 W. J. Wang, J. Zhang, S. C. Yang, B. J. Ding and X. P. Song, *ChemSusChem*, 2013, **6**, 1945.
278 J. Zhang, K. Sasaki, E. Sutter and R. R. Adzic, *Science*, 2007, **315**, 220.
279 R. Borup, J. Meyers, B. Pivovar, Y. S. Kim, R. Mukundan, N. Garland, D. Myers, M. Wilson, F. Garzon, D. Wood, P. Zelenay, K. More, K. Stroh, T. Zawodzinski, J. Boncella, J. E. McGrath, M. Inaba, K. Miyatake, M. Hori, K. Ota, Z. Ogumi, S. Miyata, A. Nishikata, Z. Siroma, Y. Uchimoto, K. Yasuda, K. I. Kimijima and N. Iwashita, *Chem. Rev.*, 2007, **107**, 3904.
280 V. R. Stamenkovic, B. Fowler, B. S. Mun, G. F. Wang, P. N. Ross, C. A. Lucas and N. M. Markovic, *Science*, 2007, **315**, 493.
281 N. Tian, Z. Y. Zhou, S. G. Sun, Y. Ding and Z. L. Wang, *Science*, 2007, **316**, 732.
282 A. Kloke, F. von Stetten, R. Zengerle and S. Kerzenmacher, *Adv. Mater.*, 2011, **23**, 4976.
283 J. Wu and H. Yang, *Acc. Chem. Res.*, 2013, **46**, 1848.
284 L.-X. Ding, A.-L. Wang, G.-R. Li, Z.-Q. Liu, W.-X. Zhao, C.-Y. Su and Y.-X. Tong, *J. Am. Chem. Soc.*, 2012, **134**, 5730.
285 X. Huang, E. Zhu, Y. Chen, Y. Li, C.-Y. Chiu, Y. Xu, Z. Lin, X. Duan and Y. Huang, *Adv. Mater.*, 2013, **25**, 2974.